Energy Environmental Science

Cite this: *Energy Environ. Sci.*, 2011, **4**, 3223

www.rsc.org/ees

REVIEW

Recent advances in the research of polyanion-type cathode materials for Li-ion batteries

Zhengliang Gong[a] and Yong Yang*[ab]

Received 25th November 2010, Accepted 31st May 2011
DOI: 10.1039/c0ee00713g

In the past decades, research efforts on polyanion-type cathode materials by the scientific community intensified significantly. This paper reviews the latest advances in the exploration and development of polyanion-type compounds as high performance cathode materials for Li-ion batteries. It focuses on the synthesis, structure and physicochemical (especially electrochemical) properties of several classes of polyanion compounds. The relationship between composition–structure–performance of the novel electrode materials is also summarized and analyzed. The main approaches, achievements and challenges in this field are briefly commented and discussed.

1. Introduction

The Li-ion battery is a type of rechargeable batteries with the highest energy density developed so far. The energy density of the developed Li-ion batteries can be as high as 250 Wh kg^{-1} and its life cycle can last for more than 10 000 cycles depending on the working conditions such as depth of charge/discharge (DOD), *etc.* However, the development of Li-ion batteries is quite diverse since there are several chemistry systems in which mainly different cathode materials are used. In fact, cathode materials play an important role in the determination of energy density, safety and life cycle of Li-ion batteries.[1,2] Therefore, research and development of cathode materials is one of the popular topics at main international meeting on Li-ion batteries. Up to now, three types of cathode materials have been investigated intensively, *i.e.* layered lithiated transition metal oxides, Mn-based spinels and polyanion-type cathode materials. Layered transition metal oxides cathode materials have several advantages: fully developed synthetic routes, high capacity and ability for facile processing. However, they all have an unavoidable shortcoming, *i.e.* oxygen evolution at high charging potential. It could cause serious safety issues for practical application. Thus layered lithiated transition metal oxides such as $LiCoO_2$ or $LiNi_{1-x-y}Co_xMn_yO_2$ ($0 \leq x, y \leq 1$) are only widely used as electrode materials in small-scale batteries for portable electronic equipments. Mn-based spinels such as $LiMn_2O_4$ have also several advantages such as low cost, environmental benignness and good thermal stability, thus it is a good candidate for cathode materials for power tools applications. Another type of cathode material are polyanion compounds such as $LiFePO_4$, which was firstly reported by J. Goodenough[3] and has been widely investigated in the last decade. The specific characteristics of $LiFePO_4$ such as cycle stability, safety, environmental friendliness and potential low cost make this material the most competent electrode material in future Li-ion batteries for plug-in hybrid electric vehicles applications. The review of the recent status of polyanion compound cathode materials is

[a]*School of Energy Research, Xiamen University, Xiamen, 361005, China*
[b]*State Key Lab of Physical Chemistry of Solid Surface & Department of Chemistry, Xiamen University, Xiamen, 361005, China*

Broader context

Due to the economic vulnerability of fossil fuels, and increasing environmental and global warming concerns, the development of alternative renewable and clean energy sources is intensively pursued worldwide. These new developments have raised a strong demand for high performance energy storage systems with increased safety and lower costs. Li-ion batteries (LIBs) have been considered as one of the most promising energy storage technologies to meet these requirements, for hybrid, plug-in hybrid, and electric vehicle applications to the reduction of CO_2 emissions arising from transportation. Extensive studies have been devoted to exploring and developing new materials for high performance LIBs. This paper give a comprehensive review of the recent research on the synthesis, structure and electrochemical performance of the main polyanion compounds as cathode materials for LIBs with high energy density, high power capability, and excellent cycling and thermal stability. Also, recent research efforts to explore polyanion materials with reversible exchange of more than one Li per formula unit for the next generation LIBs are highlighted in this paper.

imperative for the future research in this field. This paper mainly reviews the newest advances in the research and exploration of new polyanion compounds as cathode materials for Li-ion batteries. Structure, electrochemical performance and synthetic methods of the new electrode materials have been summarized and analyzed. The problems and challenges in this exciting field have also been cited and discussed.

2. Development of polyanion cathode materials

Polyanion compounds are a class of materials in which tetrahedral polyanion structure units $(XO_4)^{n-}$ and their derivatives $(X_mO_{3m+1})^{n-}$ (X = P, S, As, Mo, or W) with strong covalent bonding combine with MOx (M = transition metal) polyhedra. Polyanion cathode materials possess higher thermal stability than conventional used layered transition-metal oxides due to the strong covalently bonded oxygen atoms, which make them more suitable for large-scale Li-ion battery applications, by virtue of their better safety properties. As a new class of cathode materials for lithium ion batteries, polyanion compounds have attracted great interest since the first report on the electrochemical performance of $LiFePO_4$ by Padhi *et al.*[3] Table 1 summarizes some properties of polyanion compounds which have been investigated up to now.[4–42] The crystal structures of these typical polyanion-type cathode materials are also compared in Fig. 1.

2.1 Synthesis

To improve the electrochemical performance and decrease the cost of polyanion-type cathode materials, various synthetic routes such as solid-state reaction,[3,43,44] sol–gel processing,[45,46] solution precipitation,[47,48] hydrothermal processing,[49–51] solvothermal process,[52–54] polyol process and ionothermal[55,56] routes have been proposed and optimized. The exploration and optimization of these synthetic routes were mainly focused on the development of homogeneous polycrystalline nanoparticles with controlled particle size and/or high quality (uniform and thin) carbon coating. For iron compounds, inert gas or slightly reducing condition are required to suppress the formation of impurity Fe^{3+} phases, and moderate low sintering temperature is preferred to prevent undesirable particle growth. Carbon or some carbon-containing compounds are normally added to the precursors or the intermediate mixtures, and act as a carbon source facilitating the formation of the $LiFePO_4$/C composite, also protecting the Fe^{2+} from oxidation and inhibiting the particles growth and aggregation.

2.1.1 Solid state reaction. Solid state reaction is a traditional and widely used method for synthesis of ceramics, which includes intimate grinding and sintering of the stoichiometric mixture of starting materials. It is an economic, efficient, and easy scale up method to synthesize lithium polyanion compounds for Li-ion batteries. In general, the raw materials were firstly mixed and thoroughly ground and/or milled, then subjected to heat treatment at a temperature of 300–400 °C to expel the gases. After that, the mixture was reground and/or pelletized, then sintered at temperatures ranging from 600 to 800 °C for 10–24 h.[3,12,41] Through optimization of solid-state reaction conditions, Yamada *et al.* firstly achieved high utilization of >95% of the 170 mAh/g theoretical capacity of $LiFePO_4$ at room temperature.[43] The disadvantage of solid state reactions includes inhomogeneous composition, irregular morphology, uncontrollable particle growth and agglomeration and long heating times, followed by several grinding and annealing processes.[57,58] The undesirable particle growth and agglomeration can be prevented by adding growth inhibitors such as carbon, and nanoparticles can be obtained.[59–61]

2.1.2 Sol–gel process. The sol–gel process is a wet-chemical technique widely used in the fields of materials science and ceramic engineering. Compared to the traditional ceramic power process, it can ensure higher purity and homogeneity and small particle size due to better mixing of the reactants. In this process, the precursors were

Zhengliang Gong

Zhengliang Gong received his Ph.D. in Physical Chemistry from Xiamen University in 2007. He then worked as a postdoc research fellow at the Department of Chemical and Biomolecular Engineering, the National University of Singapore before joining the faculty of Xiamen University. His research is focuses on materials for energy storage and conversion and the electrochemical processes in these systems. His current research is fully devoted to the development of new materials for improving the energy and power density of lithium ion batteries.

Yong Yang

Yong Yang obtained his Ph.D. in Physical Chemistry at Xiamen University in 1992. Except for a one-year (1997–1998) academic visit at Oxford University, he has worked at the State Key lab for Physical Chemistry of Solid Surface at Xiamen University since 1992. Now he is a distinguished professor there. His main research interests are new materials, in situ spectroscopic techniques, interfacial and reaction mechanism study in electrochemical energy storage and conversion system. He was given the Award for outstanding young scholar research by the National Natural Science Foundation of China in 1999.

Table 1 Properties of some polyanion compounds

Polyanion compounds		Structure	Voltage/V (*vs* Li)	Theoretical capacity/ practical capacity (mAh/g)	Thermal stability	Remarks	Ref.
Phosphates	$LiFePO_4$	Olivine structure,	3.5	170/> 160	Excellent	Excellent cycling stability	3,4
	$LiMnPO_4$	orthorhombic (space group *Pmnb*)	4.1	171/160	Good	Instability of delithiated state and low cycling performance at high temperature	5–7
	$LiCoPO_4$		4.8	167/120	Poor	high electrode potential,	8–10
	$LiNiPO_4$		5.1	169/(no data)	\	practical application will rely on the development of electrolytes with higher stability window	10,11
Silicates	Li_2FeSiO_4	Li_3PO_4 structure, tetrahedral (as much as 8 polymorphs)	2.8/4.8[a]	332/200	Excellent	Possible for two electron reaction ($Fe^{2+}/Fe^{3+}/Fe^{4+}$ redox couples), good cycling stability	12–15
	Li_2MnSiO_4		4.1/4.5 [a]	333/250	\	Poor cycling stability, amorphism upon dilithiation	16–18
	Li_2CoSiO_4		4.2/5.0 [a]	325/100	\	Higher electrode potential, low electrochemical activity, poor cycling performance	19–21
Fluorophosphates	$Li(Na)VPO_4F$	Triclinic (space group $P\bar{1}$)	4.2	156/155	Excellent	Higher electrode potential, good cycling stability	22–25
	$Na_3V_2(PO_4)_2F_3$	Tetragonal (space group $P4_2/mnm$)	4.1	192/120	\	Irreversibility of extraction of the third Na^+	26,27
	$Li_5V(PO_4)_2F_2$	layered monoclinic (space group $P2_1/c$)	4.1	170 ($V^{3+}/V^{4+}/V^{5+}$) redox couples)/70	\	Poor reversibility of V^{4+}/V^{5+} redox couple	28,29
	$Li(Na)_2FePO_4F$	Layered or stacked or 3D structure was adopted depends on the alkali ion and transition metal ion	3.5	292/135	Good	two-dimensional ion conduction paths and solid-solution-like electrochemical behavior	30–32
	$Li(Na)_2MnPO_4F$		\	\	\	Electrochemical inactive	33,34
	$Li(Na)_2CoPO_4F$		5.0	287\120	Good	Both large theoretical	35,36
	$Li(Na)_2NiPO_4F$		5.3	287\(not determined)	\	capacity and high electrode potential, practical application will rely on the development of electrolytes with higher stability window	37
Fluorosulphates	$LiFeSO_4F$	Triclinic (space group $P\bar{1}$)	3.6	151\135	\	Better ionic/electronic conductivity compared with $LiFePO_4$	38–40
	$LiMSO_4F$ (M = Co, Ni)	Triclinic (space group $P\bar{1}$)	\	\	\	Electrochemical inactive	39
	$LiMnSO_4F$	Monoclinic (space group $P2_1/c$)	\	\	\	Electrochemical inactive	39
Borates	$LiFeBO_3$	Monoclinic (space group $C2/c$)	3.0	220\200	\	Solid-solution intercalation mechanism	41,42
	$LiCoBO_3$	Monoclinic (space group $C2/c$)	\	215\(no data available)	\	Almost negligible electrochemical activity	42
	$LiMnBO_3$	Hexagonal (space group $P\bar{6}$)	\	222\110	\	A plateau around 4.3 V with limited capacity, most of the capacity lie in the voltage of 1.25–4.3 V	42

[a] The voltage to extract the second lithium from Li_2MnSiO_4 (M = Fe, Mn and Co) according to the results of theoretical calculation.

firstly dissolved in solvents, and then the sol (or solution) evolved gradually towards the formation of a gel-like network containing both a liquid phase and a solid phase. Then the gel was dried and sintered at temperatures from 500 to 700 °C. For the purposes of sol–gel synthesis of polyanion cathode materials, various precursors and solvents were used. In the case of $LiFePO_4$, the precursors combined lithium, iron and phosphorus sources, such as lithium phosphate and iron(III) citrate with phosphoric acid,[62,63] lithium acetate and ferrous acetate,[45,64] lithium carbonate and ferrous oxalate,[65] lithium nitrate and ferrous oxalate[46] were used. When organic solvent/chelating agents or some carbon-based compounds (such as acetates, citrates, oxalates, *etc*.) are used, a uniform carbon coating layer is produced *in situ*.[64] Based on the consideration of preparing polyanion materials with controlled particle size and/or high quality (uniform and thin) carbon coating to improve their electrical conductivity and minimal Li-ion diffusion path length, the sol–gel method is regarded as one of the best techniques.

2.2.3 Hydrothermal/solvothermal process. The hydrothermal/solvothermal process allows to synthesize polyanion compounds

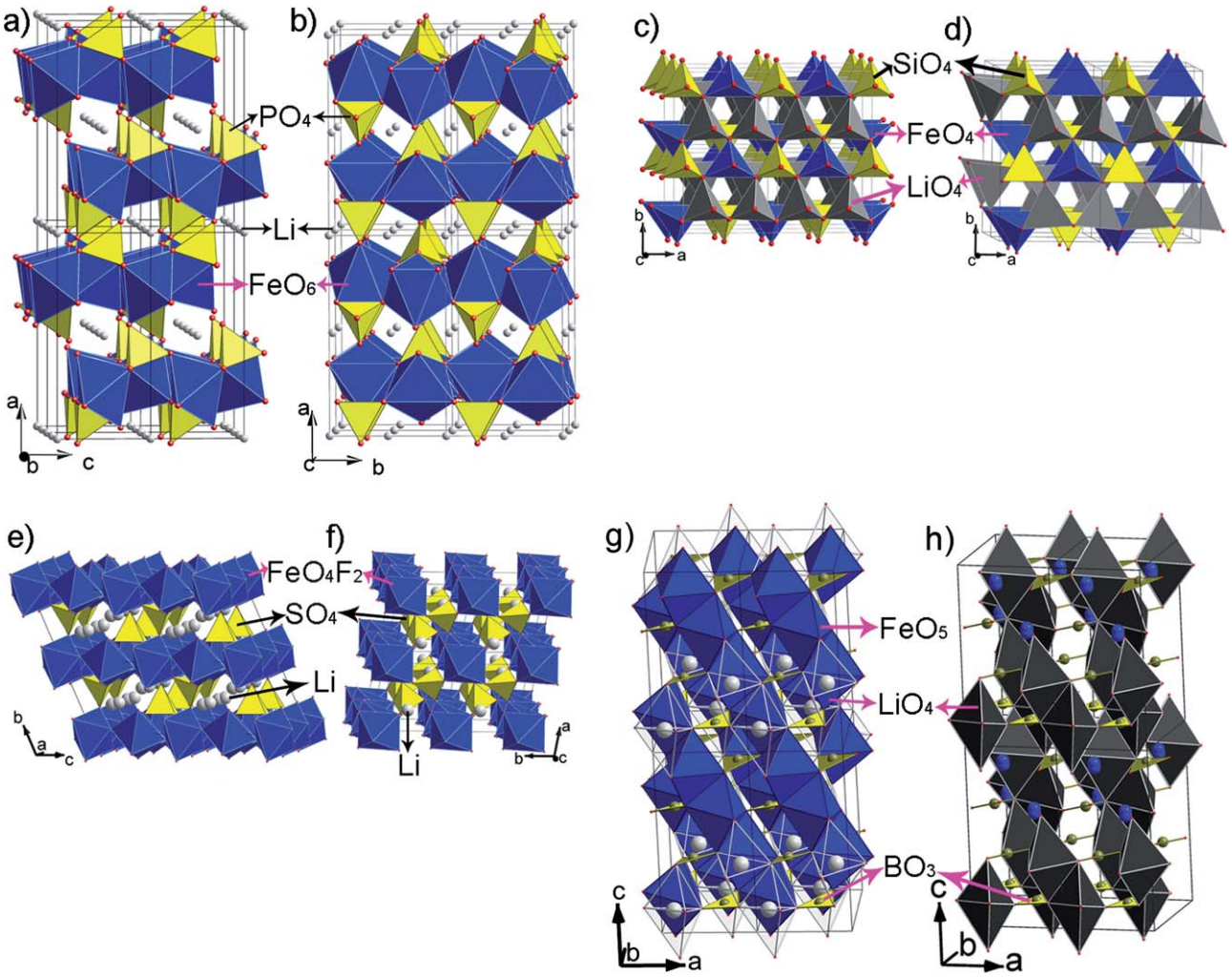

Fig. 1 Polyhedral representation of the crystal structure of some typical polyanion-type cathode materials. (a) and (b) Olivine $LiFePO_4$ viewed along the *b*- and *c*-axis, respectively. Yellow tetrahedral, PO_4; blue octahedral, FeO_6. (c) Li_2FeSiO_4 (space group $Pmn2_1$) viewed along the *c*-axis; (d) Li_2FeSiO_4 (space group *Pmnb*) viewed along the *c*-axis. Grey tetrahedral, LiO_4; blue tetrahedra, FeO_4; yellow tetrahedra, SiO_4. (e) and (f) LiFeSO4F viewed along the *a*- and *c*-axis, respectively. Yellow tetrahedral, SO_4; blue octahedral, FeO_4F_2. Li distribution between two half-occupied positions is disordered. (g) $LiFeBO_3$ viewed along the *b*-axis; (h) $LiFeBO_3$ viewed along the *b*-axis with FeO_5 bipyramid not indicated, possible Li diffusion pathways parallel to the *c*-axis are showed. The paired face-sharing LiO_4 tetrahedra are shown in grey (lithium statistically occupies two tetrahedral sites, statistically alternate positions of Li are not indicated for simplicity), trigonal FeO_5 bipyramids are shown in blue (iron statistically occupies two trigonal sites), BO_3 triangles are shown in yellow.

at relatively low temperature with well controlled morphology (*e.g.*, spherical, cubic, fibrous, and plate-like) and fine crystal particles (from a couple of nanometres to tens of microns). The morphology and particle size of the products can be tuned in a wide range, using thermodynamic variables, such as reaction temperature, pH, and concentrations of the reactants, in addition to kinetic parameters, such as speed of stirring. In this process, the reactants are dissolved in water or another solvent and sealed in an autoclave, and then hydrothermally/solvothermally processed above the boiling point of the solvent at high pressure for the desired length of time. The heating process can be performed in a conventional oven or a microwave oven. Compared to the conventional heating methods transferring heat convectively in a reactor, the microwave technology uses electromagnetic waves for heating which can transfer energy selectively to the microwave absorbing materials.[15,52,53] When a microwave oven was used, the total volume of the reactants could be heated uniformly.

However, post-heat treatment is normally required for $LiFePO_4$ synthesized by a hydrothermal/solvothermal method to eliminate the unfavorable effects of lithium/iron anti-site mixing occurring at low temperatures (*ca.* 100∼120 °C)[50] or absorbed solvents. Increase in the temperature of the hydrothermal/solvothermal process can minimize the anti-site mixing and well crystallized $LiFePO_4$ nanoparticles can be obtained if a sustainable high-pressure reactors are used.[66] Ascorbic acid, sucrose, citric acid, *etc.* are all used as reducing agents to prevent the oxidation of Fe^{2+} in aqueous environment during the hydrothermal process.[67]

2.1.4 Precipitation process. The precipitation process is also an effective solution method for preparing polyanion

compounds with high purity, homogeneity and good crystallinity. For $LiFePO_4$, the co-precipitation technique consisted of mixing Li^+, Fe^{2+}, PO_4^{3+} precursor in aqueous solution, and led to precipitation *via* adjusting the temperature and pH value to facilitate the formation of $LiFePO_4$ rather than the formation of Li_3PO_4 and $Fe_3(PO_4)_2$. The obtained precipitate was then washed with water, dried under vacuum and heat-treated at 400–700 °C.[47,68,69] The precipitation process has the advantages of a simple synthesis process and low energy consumption, which can also allow the homogeneous mixing of precursors at the atomic level. The temperature and the dwell time of calcination can be significantly reduced as compared to conventional solid-state methods, since the crystalline $LiFePO_4$ phase is already formed during the precipitation process. The precipitation process is especially suitable for synthesizing doped polyanion compounds, as the doping process of co-precipitation in aqueous solution, which can easily blend all soluble components uniformly even for low content of ion dopant.[70]

2.1.5 Polyol process. The polyol method is another promising process for obtaining fine particles with a well-defined shape and a narrow size-distribution *via* controlling the thermodynamic and kinetic variables. In general, a mixture of reaction reagents and a polyalcohol medium (such as tetraethylene glycol (TTEG), diethylene glycol (DEG), ethylene glycol (EG), *etc.*) is heated in an oil bath and refluxed for several hours. The reaction temperature lies in the range of 200–400 °C, based on the boiling point of the polyol media (314 °C for TTEG, 285 °C for triethylene glycol,and 245 °C for diethylene glycol), that intermediate between the solid state and the hydrothermal process. The polyol process is similar to the solvothermal process except for the reaction being carried out under atmospheric pressure. The polyol medium itself acts not only as a solvent to dissolve the precursors in the process but also as a stabilizer, limiting particle growth and prohibiting agglomeration, thus nanoparticles are normally obtained.[71–74] Compared to hydrothermal synthesis, more highly crystal samples are acquired directly from the reaction medium without additional sintering being necessary, because higher reaction temperature is used. Especially, the polyol process provides a reducing environment, which is highly favorable for synthesizing divalent iron containing polyanion compounds.

2.1.6 Ionothermal process. Ionothermal synthesis, the use of ionic liquids (ILs) as both solvent and template (structure-directing agent), was introduced by Recham *et al.* to prepare nanostructured polyanion cathode materials such as $LiFePO_4$,[55] Na_2MPO_4 (M = Fe, Mn, $Fe_{1-x}Mn_x$)[33] and $LiFePO_4F$,[31] *etc.* Recently, using ionothermal synthesis, a novel metastable fluorosulfate polyanion compound ($LiFeSO_4F$) was successful developed by Recham *et al.* as a promising cathode material.[38] This demonstrates the potential of ionothermal synthesis in the discovery of novel materials, especially for metastable compounds. As a new and promising method, the ionothermal synthesis has been recently reviewed in detail by Tarascon *et al.*[56,75] and so will only be briefly mentioned here. Ionothermal synthesis is similar to the inorganic molten salt synthetic method, while it uses room temperature molten salts (ILs) as a reaction medium. Many ionic liquids are relatively polar solvents, and are feasible to dissolve the inorganic reactants. The high thermal stability and very low vapor pressure properties of ILs directly result in reactors such as autoclaves or reflux condensers being unnecessary, and also make the synthesis process simple and safe. The reaction temperature, typically 150–300 °C, depends on the temperature window of the ionic liquid used. Most ionic liquids were found to be (somewhat) thermally stable up to and above 300 °C. The physico-chemical properties of ILs—such as interaction with inorganic reactants, viscosity, melting point, and acidity—could be adjusted by changing the organic anion and cation. A proper choice of organic anion and cation is critical for a successful synthesis with the ionothermal process. It was reported that the particles morphology of the obtained products can be tuned by choosing the proper ILs and introducing some additives such as diol, although the detailed mechanism is not yet fully understood. The high cost drawback of ILs can be overcome in principle by recovery.

2.2 Electronic structure

The performance of the Li-ion batteries is directly related to the crystal structure/electronic structure of the electrode materials, which govern the electronic/ionic transport properties, cell potential and the number of exchanged electrons. Information on the intrinsic electronic conductivity can be directly inferred from the electronic structure of the electrode materials. The coulomb correlation, the charge transfer energy, the hybridization strength between the cation 3*d* and oxygen 2*p* states and the crystal field splitting for the $d^n p^m$ configuration of the transition metal-oxygen tetrahedral, control the ground state electronic structure, magnetic and transport properties of the cathode materials for lithium-ion batteries. In polyanion-type cathode materials, the valence electrons of transition metals tend to be isolated from that of polyanion, thus the electronic structure of these materials is governed mainly by isolated transition metal-oxygen polyhedral groups.[76] Although the inductive effect generated by the polyanionic groups leads to a higher operating voltage than that in oxides,[3,8,77] the polyanionic groups simultaneously isolating the valence electrons of transition metals lead to the observed low electronic conductivities.[1,8,78] Understanding the electronic structure of polyanion compounds plays a very important role in the practical usage of the lithium ion battery. Extensive studies have been devoted to both theoretical and experimental studies of their electronic structure, in order to understand well the related properties, such as electronic conductivity, magnetic properties, the reaction mechanism of the electrochemical process, lithiation/delithiation potential, the effect of doping element on the electronic properties, *etc.*[13,79–88] For the theoretical study of the electronic structure, the first principles methods based on the density functional theory (DFT) in the local spin-density approximation (LSDA) or the generalized gradient approximation (GGA) were widely applied. Experimentally, optical/photoelectron spectroscopy and magnetic susceptibility measurements are a powerful experimental tool for investigating the electronic structure of materials for lithium-ion batteries. Both electronic conductivity measurements and optical spectroscopy studies show that most of these polyanion-type cathode materials (such as $LiMPO_4$, Li_2MnSiO_4 and $LiMSO_4F$; M = transition metal) are wide-band-gap (band

gap normally high than 3 eV) insulators.[38,81,89,90] However, using only LDA/GGA methods is shown to cause large errors in predicting the electronic structure and generally predicting semiconductor/semimetal behavior, due to their inability to capture precisely the coulomb correlation effects that are important for the d-electrons of the transition-metal elements.[91,92] Using the DFT + U method, more accurate treatment of the Coulomb correlations can be obtained. In this method, the Coulomb correlation among electrons on a single M (or other transitional metal) site is explicitly included in the total energy functional in a way similar to the U-term in the Hubbard-like model.[93] The results of DFT + U calculations are in fairly good agreement with experiments for the Li intercalation potential, lattice parameters, and energy gap for these polyanion compounds.[81,85,87,88,91,92]

2.3 Phosphates

The polyanion cathode materials most intensively investigated are phosphates ($LiMPO_4$, with M = Fe, Mn, Co or Ni) with ordered olivine structure. The literature on phosphates is very extensive and is only briefly summarized here. For more details, a number of review articles are available.[94–99]

The olivine-type structure of $LiMPO_4$ (Fig. 1a and 1b) can be described as a slightly distorted hexagonal close-packed (hcp) oxygen array resulting in an orthorhombic structure (D_{2h}^{16}-space group *Pmnb*).[3] Within the hcp oxygen framework, Li and M metal atoms are located in half of the octahedral sites and P atoms are located in 1/8 of the tetrahedral sites. The MO_6 octahedra share corner forming zigzag chains running parallel to the *c*-axis in the alternate *a*–*c* planes. These chains are bridged by corner- and edge-sharing PO_4 tetrahedra to form a host structure with strong three dimensional bonding. The LiO_6 octahedra share edge forming linear chains running parallel to the *c*-axis in the other *a*–*c* planes, and Li^+ ions form one dimensional tunnels in the host structure along the [010] direction that run parallel to the planes of corner-sharing FeO_6 octahedra.

$LiFePO_4$ is the most widely studied and fully developed material among olivine phosphates, and is generally considered to be one of the most promising battery materials used in Plug-in Hybrid Electric Vehicle/Electric Vehicle (PHEV/EV). The application of iron-based compounds as a cathode for lithium batteries shows several advantages, including abundant cheap raw materials, high thermal stability and relatively low toxicity. However, the iron-based oxides containing O^{2-} as the anion suffer problems for the cathode designer, as in these oxides the Fe^{4+}/Fe^{3+} redox energy tends to lie too far below the Fermi energy of a lithium anode while the Fe^{3+}/Fe^{2+} couple is too close to it. The strong covalent bonding within the $(PO_4)^{3-}$ polyanion reduces the covalent bonding to the iron ion, which lowers the Fe^{3+}/Fe^{2+} couple redox energy to a suitable level of a flat voltage of 3.4 V *versus* Li/Li^+.[3] Besides its suitable high operating voltage, $LiFePO_4$ possesses appreciable theoretical capacity (*ca.* 170 mAh/g), corresponding to the theoretical energy density 580 Wh kg^{-1} *versus* Li electrode, which above the practical value of $LiCoO_2$ (supposing that only 0.5 Li^+ can be cycled in Li_xCoO_2).[100] $LiFePO_4$ also has high thermal stability in both lithiated and delithiated states, which enables the batteries to stably operate at higher temperatures and to be safe even under harmful conditions. The slight volume change (6.81%) of $LiFePO_4$ upon de/lithiation guarantees good structure stability, and thus exhibits excellent cycling reversibility.[3] Furthermore, $LiFePO_4$ triphylite is a naturally occurring mineral abundant in nature and iron is a non-toxic element, which makes it environmentally friendly, and the plentiful raw materials reduce its final product cost. Now, the intrinsic drawbacks of low conductivity can be partly conquered by surface conducting coatings combined with particle-size reduction and aliovalent doping. These factors make it an amazing cathode material for high-power Li-ion battery systems today. Therefore, a number of companies worldwide start to invest in research and development $LiFePO_4$ batteries, and the production of $LiFePO_4$ batteries has expanded dramatically in recent years. Several prototypes of hybrid and plug-in hybrid vehicles equipped with $LiFePO_4$ batteries have already been demonstrated by several automobile companies. As one of the most promising cathode materials for high-power batteries, $LiFePO_4$ has attracted a great deal of scientists' attention and been studied extensively.

Despite the many advantages associated with $LiFePO_4$, there are some drawbacks with $LiFePO_4$; the key drawbacks for the commercial application are its low intrinsic electric conductivity ($\sim 10^{-9}$ S cm^{-1}),[78] low packing density and poor one dimension lithium ion diffusion.[101] In the past decade, many studies have been conducted in an attempt to overcome this problem. These have mainly been concentrated on optimizing the synthetic strategy,[43,49] surface conducting modification,[60,102] particle size reducing,[103,104], cation doping on lithium and/or iron sites,[78,105,106] and so forth.

Surface modification has been widely used to improve the electronic conductivity of $LiFePO_4$, since the initial work by Ravet *et al.*,[59] who reported an improved electrochemical performance of $LiFePO_4$ *via* a synthesis leading directly to carbon-coated particles. Carbon is the most popular coating material for polyanion electrode materials to improve their low intrinsic electronic conductivity. Besides improving the conducting of $LiFeO_4$/C particles, the presence of carbon can also act as a reducing agent to prevent the formation of Fe^{3+} impurity phase, isolate the $LiFeO_4$ particles to suppress the undesirable particle growth and aggregation.[107] However, the presence of carbon also reduces the volumetric energy density of the electrode, which may affect its practical application. Thus, the key point of the carbon coating process is to form a thin coating layer with high conductivity by an economic procedure. Various carbon sources have been proposed to form the carbon coating layer, *e.g.*, sucrose,[59] resorcinol-formaldehyde gel,[60] carbon black,[108] white table sugar,[109] naphthalenetetracarboxylic dianhydride,[110] hydroxyethylcellulose, [111] polypropylene,[57] and so forth. Studies on the effects of the structure of residual carbon produced from different organic precursors showed that sp^2-coordinated carbon exhibits better electronic properties than disordered or sp^3-coordinated carbonaceous materials.[112–114] Other non-carbonaceous coating layers, such as metallic conducting layer[115,116] and conductivity polymer films[52,117,118] were also found able to enhance the performance of $LiFePO_4$. Recently, an ultra-high rate performance of $LiFeO_4$ was reported by Kang and Ceder, creating a fast ion-conducting lithium phosphate glass layer on $LiFePO_4$ particle surface through controlled off-stoichiometry.[119] However, the ultra-high rate

capability and the cause of the excellent performance of their samples were extensively questioned by Zaghib *et al.* and further discussed.[120,121]

Recently, graphene, a two-dimensional aromatic monolayer of a carbon atom, is widely studied as electrode material for lithium ion batteries, due to its excellent mechanical and electronic properties, such as superior electrical conductivity, high specific surface area (2630 m^2 g^{-1}), high values of Young's modules, fracture strength, room temperature quantum Hall effect, and mimic massless transportation properties.[122–124] Such merits also make graphene sheets promising matrices for metals and metal oxides to improve their electrochemical performance.[125–127] Highly reversible capacities and good cycle performances were achieved when oxides/graphene, carbon nanotube/graphene, and fullerene/graphene composites were used as anode materials for lithium ion batteries. Its high surface area and outstanding electrochemical properties also suggest that graphene holds promise as a highly efficient conductive additive with much less mass fraction for polyanion-type cathode materials to improve their electronic conductivity.[128–131] For example, the graphene character (*e.g.* sp^2/sp^3 ratios) of the carbon coating layer was found to affect significantly the conductivity of $LiFePO_4$/C composites.[113,114,132] Higher graphene character results in higher composite conductivities, and thus higher rate capabilities of the composites. For example, Ding *et al.* used graphene nanosheets as additives to improve the electronic conductivity of $LiFePO_4$/graphene composites.[129] The as prepared $LiFePO_4$/graphene composites exhibit remarkably enhanced capacity delivery and cyclability with only 1.5 wt% of graphene, with an initial discharge capacity of 160 mAh/g at 0.2 C and the capacity value remained 110 mAh/g even at the high rate of 10 C. Su *et al.*[130] demonstrated that, compared to commercial carbon based additives, graphene nanosheet additives can achieve better electrochemical performance with much less mass fraction for the LiFePO4 cathode, based on both laboratory-based experimental coin cells and commercial battery packs.

The effect of cationic aliovalent doping on the conductivity of $LiFePO_4$ has been a highly debated topic in the studies of $LiFePO_4$ materials with an ample amount of points both for[78,82,133–136] and against[106,137–142] the argument. More than 10^8 times increase in electronic conductivity was reported for $Li_{1-x}M_xFePO_4$ (M = Mg, Al, Ti, Nb or W) with low-level supervalent ions doped into the Li 4a site by Chung and co-workers.[78] The introduction of p-type and n-type conductivity at the fully discharged and charged state was suggested responsible for this dramatical conductivity increase. However, poor conductivity for Zr- and Nb-doped $LiFePO_4$ was showed in a subsequent study.[137] Other studies on doped (and undoped) $LiMPO_4$ (M = Fe, Ni) show that a percolating nano-network of metal-rich phosphides may be responsible for the enhanced conductivity.[138,139] Further investigation is needed to understand the exact mechanism for aliovalent doping to improve the electronic conductivity after carefully deducting the effects of the impurity phase on the electrochemical performance of doped materials.

Initially, a strictly $LiFePO_4/FePO_4$ two-phase reaction mechanism was postulated for $LiFePO_4$ according to its extremely flat charge/discharge profile.[3] It was generally believed, on the basis of the Gibbs phase rule, that lithium extraction/insertion proceeds by varying the $FePO_4/LiFePO_4$ ratio in the whole range of x in $LixFePO_4$. Solid solution behavior was clarified in subsequent studies,[103,143,144] and the miscibility gap between the two monophases $Li_\alpha FePO_4$ and $Li_{1-\beta}FePO_4$ (α and β close to zero) was found to depend both on temperature,[145] particles size[135,146–148] and doping.[134] The existence of single phase domains, $Li_\alpha FePO_4$ and $Li_{1-\beta}FePO_4$ phases, close in composition to the end-membranes $LiFePO_4$ and $FePO_4$, was also predicted by theoretical calculation and modeling.[143] Solid solution behavior was first observed in the Fe^{3+}/Fe^{2+} redox reaction region of $Li_xMn_{0.6}Fe_{0.4}PO_4$ by Yamada *et al.*[103] Using a variation temperature XRD measurement, the existence of complete solid solution in Li_xFePO_4 over the entire compositional domain ($0 < x < 1$) was observed at temperatures above 520 K.[145] The existence of narrow monophase ($Li_\alpha FePO_4$ and $Li_{1-\beta}FePO_4$) regions close to the stoichiometric end members of $LiFePO_4$ and $FePO_4$ at room temperature was then observed by Yamada *et al.* using neutron diffraction and electrochemical measurement methods.[144] The size dependence of the miscibility gap was revealed by Meethong *et al.*[135] Further, a single-phase reaction in the whole region of Li_xFePO_4 was reported in hydrothermal synthesized samples with an average particle size of 40 nm by Gibot *et al.*[146] The biggest characteristics of their sample lies in the very large amount of Li/Fe site mixing/disorder.

Generally, the value of the diffusion coefficient in $LiFePO_4$ was considered to be relatively low (varies within 10^{-10}-10^{-16} cm^2 s^{-1} depending on measurement techniques and the lithium content in solid solution $Li_\alpha FePO_4$ and $Li_{1-\beta}FePO_4$ or the $LiFePO_4/FePO_4$ phase ratio). In the earlier studies of $LiFePO_4$, reversible extraction/insertion of lithium was postulated to occur in two dimensions according to its structure features.[3] Further studies using both theoretical and experimental methods, indicated that lithium diffusion in the olivine crystal structure occurs through one-dimension channels along the [010] direction.[106,149–151] Using first-principles methods, Morgan *et al.*[149] firstly suggested that Li mobility in $LiMPO_4$ is high through 1D channels along the *b*-axis with little possibility of crossing between channels. Using empirical potential models, Islam *et al.*[106] got similar conclusions that the lowest energy pathway for Li transport is in the [010] direction. Lithium ion migration *via* a nonlinear, curved trajectory between adjacent Li sites is also predicted. By performing maximum entropy method (MEM) modeling to simulate neutron diffraction data of $Li_{0.6}FePO_4$ at 620 K, Nishimura *et al.*[150] confirmed the one-dimensional curved lithium diffusion path along the [010] direction in Li_xFePO_4. The probability density of lithium nuclei was found to strictly distribute into continuous curved pathways, *via* tetrahedral interstitial sites, along the [010] direction.

A simple shrinking core-shell model was initially postulated to depict the Li extraction/insertion processes based on the two-phase reaction mechanism of $LiFePO_4$, [3] according to which, a two-phase interface separates the $LiFePO_4$ core region from the $FePO_4$ shell and the extraction/insertion reactions proceed by the motion of the interface. Further studies revealed that the Li extraction/insertion processes are more complicated,[152,153] and some new mechanisms such as "mosaic model"[154] and "domino-cascade model",[155] *etc.* were proposed to explain the experimental observations. Recently, Delmas *et al.*[155] observed the coexistence of fully lithiated and fully delithiated individual

particles, *via* characterization of the electrochemically delithiated nanomaterials by X-ray diffraction and electron microscopy. Accordingly, they proposed a 'domino-cascade model' to describe the Li extraction/insertion mechanism, which suggests the lithiation/delithiation of each particle would be so fast that each particle should either be totally lithiated or totally delithiated. In this scheme, when lithiated/delithiated to Li_xFePO_4 the powder would be made of a fraction x of $LiFePO_4$ particles and a fraction $(1 - x)$ of $FePO_4$ particles.

The olivine $LiMnPO_4$ is isostructural with $LiFePO_4$. $LiMnPO_4$ appears to be more attractive as cathode material than $LiFePO_4$ due to its higher operating voltage (4.1 V *vs.* Li/Li^+) and similar theoretical electrochemical capacity (170 mAh/g) with $LiFePO_4$.[3] However, it suffers from very low intrinsic electrical conductivity and the large lattice distortions induced by Jahn–Teller effect from the Mn^{3+} ions. The electrical conductivity of $LiMnPO_4$ is found to be much lower than $LiFePO_4$ ($\sim 10^{-14}$ S cm^{-1} of $LiMnPO_4$ compared to $LiFePO_4$ $\sim 10^{-9}$ S cm^{-1}).[156] As a result, it has shown to deliver a very low capacity and poor rate capability.[3,5,73,157,158] To improve the performance of $LiMnPO_4$, various synthetic routes were applied to produce $LiMnPO_4$ materials with small particle size and conducting coating layer.[5,157,159–162] Recently, Bakenov *et al.*[161] prepared a $LiMnPO_4$/C composite cathode material synthesized by a combination of spray pyrolysis and wet ball milling. The obtained material shows a discharge capacity of 149 mAh/g ($\sim$ 87% of the theoretical value) at 0.1 C with good cycling stability. Mn-site substitution is proposed to enhance its cathode performance; however, it decreases the availability of the high voltage Mn^{3+}/Mn^{2+} redox couple and, consequently, lowers the capacity at 4.1 V.[103,163–166] Surprisingly, in contrast to other cations substitution (such as Mg^{2+}, Fe^{2+}, Zr^{4+}, *etc.*), Ca^{2+} substitution was found to negatively affect the electrochemical properties.[164]

Different from the high thermal stability of $LiFePO_4$ at both lithiation and delithiation states, the delithiated phase Li_yMnPO_4 (which contains a small amount of residual lithium) is relatively unstable and reactive toward a lithium-ion electrolyte.[7] Upon heating, Li_yMnPO_4 decomposes to form a new phase $Mn_2P_2O_7$, and release oxygen. Besides the low thermal stability, the cyclic stability of $LiMnPO_4$-based materials at high temperature ($\sim$ 60 °C) also needs careful consideration in practical application due to Mn dissolution in the electrolyte.

$LiMnPO_4$ also exhibits larger volume change (9.5%) between two end phase, $LiMnPO_4$ and $MnPO_4$, compared to $LiFePO_4$ (6.8%).[163] The cation substitution of Mn was found to reduce this volume change (such as 7.8% for $LiMn_{0.9}Mg_{0.1}PO_4$) due to incomplete removal of lithium upon dilithiation. Meethong *et al.*[167,168] suggested that the misfit at the phase boundary between Li-rich $Li_{1-x}MPO_4$ and Li-poor Li_yMPO_4 phase is larger for Mn phases (*ca.*10%) than that for iron phases (*ca.* 6.6%) due to the Jahn–Teller effect of Mn^{3+} ions. They concluded that the larger crystalline misfit strains play an important role in the poor electrochemical performance of $LiMnPO_4$.

The development of $LiMnPO_4$ for practical cathode application still remains a challenge for researchers, though the electrode performance of $LiMnPO_4$ has been improved significantly in recent years. Fe-doped $LiFe_xMn_{1-x}PO_4$ may be a practical choice for the application.

The high electrode potential of $LiCoPO_4$ and $LiNiPO_4$ (4.8 V and 5.1 V *vs.* Li/Li^+, respectively) makes them very attractive as cathode materials for high energy batteries.[8,10,11] However, the studies on the electrochemical performance of $LiCoPO_4$ and $LiNiPO_4$ are scarcely due to decomposition of the most commonly used electrolytes at such a high voltage. Two plateaus were observed for Li_xCoPO_4 during the charge-discharge process, which are related to two two-phase reactions within a three phase system ($LiCoPO_4$, the intermediate phase Li_zCoPO_4 and $CoPO_4$).[76,169–171] The intermediate phase, Li_zCoPO_4, was initially determined as $Li_{0.7}CoPO_4$ and recently modified to $Li_{0.6}CoPO_4$.[170] Li_zCoPO_4 was formed upon delithiation and then transformed to $CoPO_4$. The fully delithiated phase, $CoPO_4$, was found to be unstable at room temperature and to rapidly change to amorphous. The delithiated $Li_{1-x}CoPO_4$ phases have very low thermal stability and decompose upon heating in an inert atmosphere at low temperature (< 200 °C).[171] The electrochemical performance of $LiNiPO_4$ is hard to test due to its high redox potential, which exceeds the stable limitation of currently available electrolytes. The practical application of $LiCoPO_4$ and $LiNiPO_4$ will rely on the development of electrolytes with high oxidation resistance (such as ionic liquids, *etc.*).

2.4 Silicates

After the successful application of phosphates in lithium ion batteries, orthosilicates (Li_2MSiO_4, M = Fe, Mn, Co, Ni) are obviously another class of polyanion type cathode candidates with high potential. One of the approaches to increase the capacity of cathode comes from the development of materials that could afford more than one electron reversible exchange per transition metal (TM). Orthosilicates would be an ideal framework to fulfill such an option, as the $(SiO_4)^{4-}$ group would theoretically allow the 3d metal to change its valence between +2 to +4 resulting in two lithium de-/intercalation per formula unit (p.f.u.). Due to its remarkable privilege, orthosilicates have attracted great interest from researchers. Despite intensive research efforts having been devoted to this area, limited achievement has been attained on the quest for a reversible two lithium reaction in Li_2MnSiO_4 until now.

Although as novel cathode materials Li_2MSiO_4 attracted researchers' attention in 2000,[172] the appreciable cathode performance was first reported by Nyténa *et al.* in 2005.[12] Consistent with phosphate, its key limitations have been extremely low electronic conductivity and slow lithium-ion diffusion, which is believed to be intrinsic to polyanion compounds. Similar approaches to improve the conductivity of $LiFePO_4$ are also used to lithium orthosilicates.

Li_2MSiO_4 are compounds related to the Li_3PO_4 structure and belong to the large family of tetrahedral structure materials which exhibit rich polymorphism.[21] Generally, this structural type consists of approximately hexagonal close packed anions with cations in half of the tetrahedral sites, and thus face sharing between the pairs of tetrahedral sites is avoided.[173] As much as 8 different polymorphs are known for these tetrahedral structures to date, and they exist in two main classes, labeled as β and γ, according to the distribution of cations over the two possible sets of available tetrahedral sites. For β phases, all the tetrahedra are aligned in the same direction, perpendicular to the close-packed planes, and share only corners with each other (Fig. 1c), whereas for γ phases, the tetrahedra are arranged in groups of

three with the central tetrahedron pointing in the opposite direction to the outer two, with which it shares edges (Fig. 1d). The β and γ polymorphs correspond to the low and high temperature forms for a given compound, respectively. The transformations between β and γ involve a transfer of half the tetrahedral cations from occupied sites to empty ones.[174] Several variants (named β_I, γ_0, γ_{II}, *etc.*) exist for both β and γ, involving either ordering or distortions of the parent structures. A mixture of different polymorphism may be obtained during the synthesis of Li_2MSiO_4 materials due to the very small differences in formation energies of Li_2MSiO_4 polymorphisms. Some polymorphisms have been isolated *via* controlling the temperature and pressure of the synthesis and post-treatment of the materials, and the complete crystal structures have been solved.[175–181] Table 2 shows the polymorphism structures with cell parameters and a space group of Li_2MSiO_4 reported so far.

To study the structure of various Li_2MSiO_4 polymorphs, XRD and neutron powder diffraction were used as powerful tools to investigate the long-term structure, and Li MAS NMR was found to be a very sensitive tool for studying the local structure.[178,182,183] Studies on the electrochemical properties of three Li_2CoSiO_4 polymorphs (β_I, β_{II} and γ_0) indicated that the crystal structural differences have a minor effect on the lithium extraction/insertion potentials.[21] The influence of the crystal structure on the electrochemical performance of Li_2MnSiO_4 was investigated through theoretical calculations.[147] The effects of the crystal structure on the average lithium intercalation voltage for the two electron process was found to be small, GGA + U calculated voltages (according to the reaction: Host-Li_2MnSiO_4 ↔ Host-$MnSiO_4$ + 2 Li) are 4.18, 4.19, and 4.08 V for *Pmnb*, $Pmn2_1$ and $P2_1/n$, respectively.

The magnetic properties of Li_2MSiO_4 were studied by means of magnetic measurements and NMR spectroscopy.[14,184–186] The temperature dependence of the inverse magnetic susceptibility for Li_2FeSiO_4 (M = Fe, Mn, $Mn_{0.5}Fe_{0.5}$, Co) is shown in Fig. 2.[186] All studied lithium orthosilicate compounds exhibit a Curie–Weiss type dependence on temperature. An antiferromagnetic ordering appears at low temperatures due to long range M-*O*-Li-*O*-M interactions. The effective magnetic moments and the Weiss constants provided by linear fits are comparable to the theoretical spin-only values (Table 3).

As the Fe^{3+}/Fe^{4+} redox couple is hard to access, the theoretical capacity of Li_2FeSiO_4 is only 166 mAh/g based on the redox

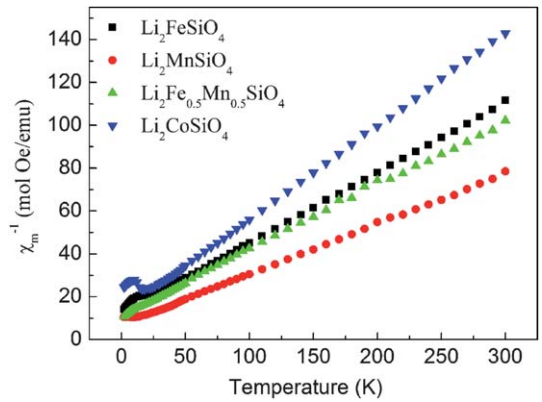

Fig. 2 Temperature dependence of the inverse molar magnetic susceptibility $1/\chi_m$ for Li_2MSiO_4 (M = Fe, Mn, $Mn_{0.5}Fe_{0.5}$, Co) prepared by a hydrothermal assisted sol–gel process (adapted from ref. 186.).

reaction $Li_2FeSiO_4 \rightarrow LiFeSiO_4 + Li^+ + e^-$. A first testing revealed that de-/lithiation processes in Li_2FeSiO_4 are highly reversible with a reversible capacity around 130 mAh/g cycled at 60 °C at a C/16 rate.[12] Fig. 3 shows the voltage profile of Li_2FeSiO_4 cycled at 60 °C. A shift of the potential plateau from 3.10 V to 2.80 V was observed between the first the second cycle, which is suggested to be related to a structural rearrangement to a more stable structure by Nyten *et al.*[12,187] Some of the Li ions (in the 4b site) and Fe ions (in the 2a site) interexchange during this rearrangement which was suggested by *in situ* XRD and *in situ* Mössbauer spectroscopy inspection.[187] Some electrochemical inactive impurity phases were observed in the as-prepared Li_2MSiO_4 materials.[12,16] Similar to $LiFePO_4$, polyanion Li_2MnSiO_4 materials possess very low intrinsic conductivity ($\sim 5 \times 10^{-16}$ S cm^{-1} for Li_2MnSiO_4 and $\sim 6 \times 10^{-14}$ S cm^{-1} for

Table 3 The Curie–Weiss constants and the effective magneton number for Li_2MSiO_4[186]

	T_N (K)	θ_p (K)	*Cp* (emu K mol^{-1})	p_{eff}
Li_2FeSiO_4	20	−38.1	3.06	4.97
Li_2MnSiO_4	12	−29.4	4.25	5.85
$Li_2Mn_{0.2}Fe_{0.8}SiO_4$		−36.8	3.13	5.03
$Li_2Mn_{0.5}Fe_{0.5}SiO_4$		−39.3	3.32	5.18
Li_2CoSiO_4	18	−31.49	2.54	4.32

Table 2 Unit cell parameters reported for polymorphs of Li_2MSiO_4 with M = Fe, Mn, Co

	Space group	*a*/Å	*b*/Å	*c*/Å	*β*/°	Ref.
Li_2FeSiO_4	$Pmn2_1$	6.26	5.32	5.01	90	12
	Pmnb	6.285	10.659	5.036		175
	$P2_1/n$	6.2835	10.6572	5.0386	89.941	175
	$P2_1$	8.229	5.0200	8.2344	99.203	176
	$P2_1/n$	8.2253	5.0220	8.2381	99.230	177
Li_2MnSiO_4	$Pmn2_1$	6.31	5.38	4.96	90	17,178
	Pmnb	6.3126	10.7657	5.0118	90	178
	$P2_1/n$	6.33	10.91	5.07	90.99	178,179
Li_2CoSiO_4	$Pmn2_1$	6.253	10.685	4.929	90	21
	$Pbn2_1$	6.2599	10.6892	4.9287	90	180
	Pmnb	6.20	10.72	5.03	90	21
	$P2_1/n$	6.284	10.686	5.018	90.60	181

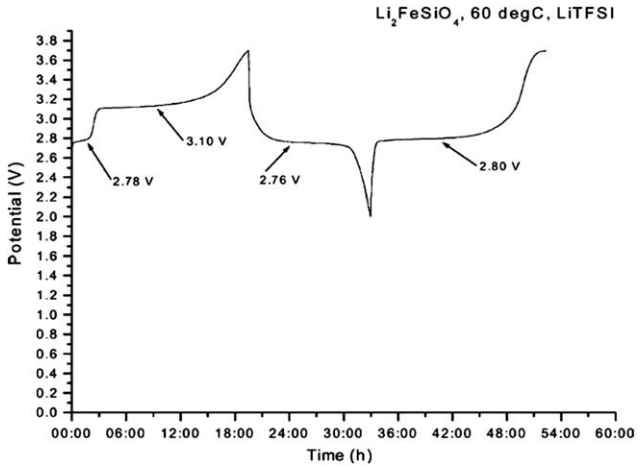

Fig. 3 A voltage profile of pristine Li_2FeSiO_4 cycled at 60 °C at a C/16 rate using 1 M LiTFSI in EC:DEC 2 : 1 electrolyte (from ref. 12.).

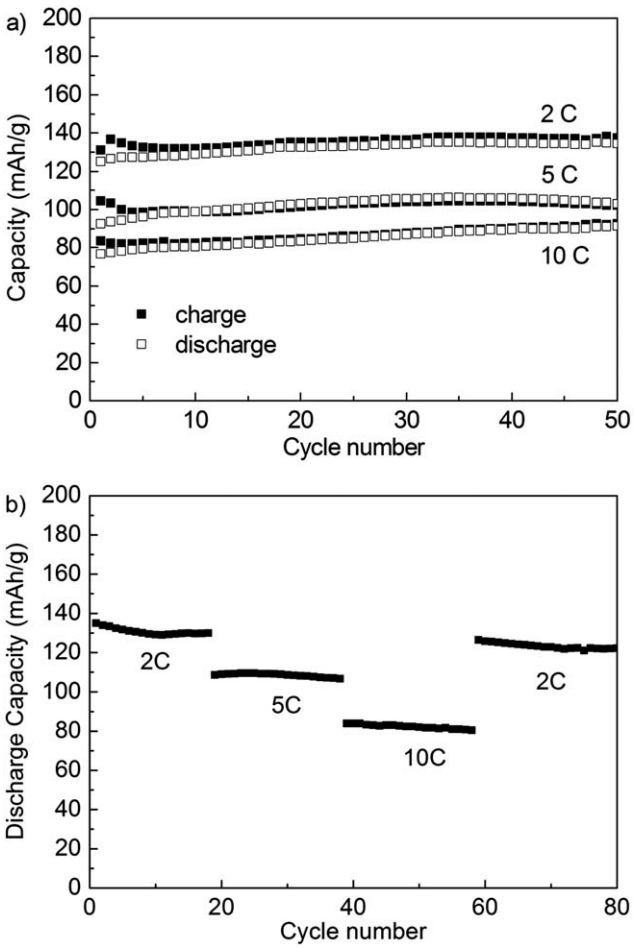

Fig. 4 (a) Cyclic performance at various charge–discharge rates; (b) reversible capacities during continuous cycling at various charge–discharge rates of Li_2FeSiO_4/C prepared by a hydrothermal-assisted sol–gel process (from ref. 14.).

Li_2FeSiO_4 at room temperature).[188] The presence of impurity phases combined with their extremely low conductivity may be of the main reasons contributing to the relatively low electrochemical activity in the early study (*e.g.* 130 mAh/g; 78% of the theoretical value).[12] To improve the electrochemical performance of Li_2FeSiO_4, various preparation processes to control the particle size and surface coating techniques to increase the electric conductivity were performed.[14,188–191] A carbon-coated Li_2FeSiO_4 material with uniform nanoparticles (approximately 40–80 nm in diameter) was synthesized by a modified sol–gel synthesis route, *i.e.*, hydrothermal-assisted sol–gel process, with sucrose added to the synthetic precursor.[14] XRD and magnetic experiments results confirmed the high phase purity of this material. Compared with the sample prepared by conventional sol–gel process, this Li_2FeSiO_4 shows superior electrochemical performance with both high rate capability and excellent capacity retention. It delivers a discharge capacity of 160 mAh/g cycled at C/16 rate at 30 °C, corresponding to 96% of the theoretical value (Fig. 4). Intriguingly, Zaghib *et al.*[184] didn't observe the potential plateau shift on their Li_2FeSiO_4 sample prepared by solid state reaction. The cyclic voltammogram results showed a delithiation voltage of 2.8 V for the first cycle. Although the authors attribute this to the high purity of their sample, further studies are required to understand the detailed mechanism for this phenomenon. According to theoretical calculation results, extracting the second lithium from Li_2FeSiO_4 will proceed at 4.8 V, with a large voltage step at the composition $LiFeSiO_4$, due to the high stability of the closed-shell d^5 ion (Fe^{3+}). Thus, it is hard to extract the remaining lithium from $LiFeSiO_4$, which implies the rarely encountered electrochemical oxidation of Fe^{3+} to Fe^{4+}. Surprisingly, when cycling at 55 °C, a capacity of 204 mAh/g with good cyclability for Li_2FeSiO_4 was recently obtained by Muraliganth *et al.*,[15] suggesting the feasibility of the reversibly extracting/inserting part of the second lithium which involved the $Fe^{3+}/^{4+}$ couple at high temperatures. By carefully optimizing synthesis process, Yang's group found that when cycling at room temperature, Li_2FeSiO_4 could also deliver high capacity corresponding to more than one lithium ion reversible extraction through charging to a high voltage of 4.8 V.[192] Furthermore, a similar result was also confirmed by the *in situ* X-ray absorption near edge structure (XANES) research on $Li_2Fe_{0.5}Mn_{0.5}SiO_4$, *i.e.*, the $Fe^{3+}/^{4+}$ redox couple was found to involve in the electrochemical reaction at a high voltage and to contribute to the observed high capacity.[193] Further exploration of the $Fe^{3+}/^{4+}$ couple would be very interesting, which would largely increase the capacity of some iron based polyanion cathode materials (such as Li_2FeSiO_4, and Li_2FePO_4F, *etc.*).

The surface stability of Li_2FeSiO_4 exposed to air and cycled with different electrolytes was studied by X-ray photoelectron spectroscopy (XPS).[194] Lithium was found to be withdrawn from the original structure of Li_2FeSiO_4 on exposure to air. Compared with electrodes stored under inert atmosphere, large amounts of carbonate-based compounds (Li_2CO_3 or $LiHCO_3$) were observed on the surface of Li_2FeSiO_4 electrodes exposed to air. When cycled with EC/PC electrolyte with LiTFSI salt, high salt stability and good cycling stability were observed.[194] Only small amounts of solvent reaction products (mainly of Li-carboxylate type) were observed on the electrode surface, neither carbonates nor LiF was found. The amount of carboxylic/carboxalate bonding is strongly enhanced when cycled with the EC/DEC electrolyte system.[195] This may indicate the formation of

a dynamic and even reversible SEI coverage, depending on the state of charge/potential of the electrode. When cycled with EC/PC electrolyte with $LiPF_6$ salt, electrolyte-induced formation of LiF and degradation of the Li_2FeSiO_4 particle surface by HF were found.[195]

At first sight, Li_2MnSiO_4 would be more attractive compared with Li_2FeSiO_4, since the higher oxidation state (+4) of Mn is more accessible than Fe. This would allow the extraction/insertion of two lithium ions, with the generation of 333 mAh/g theoretical capacity based on $Mn^{2+}/Mn^{3+}/Mn^{4+}$ redox couples.[16,17,196] So far, however, high discharge capacity (209 mAh/g, corresponding to 1.25 electrons exchange per formula unit) was only attained on the first cycle with sever capacity loss for subsequent cycles.[17] Fig. 5 shows the electrochemical performances of the material. Li_2MnSiO_4 shows a flat charge recovery at around 4.2 V and then a slope charge recovery to 4.8 with high charge-discharge polarization. A change in the shape of the charge-discharge curves was observed on subsequent de-/lithiation cycles, accompanied by irreversible capacity loss. XRD and IR results showed an irreversible change from crystalline Li_2MnSiO_4 to an amorphous state during the first charge process.[17,188,197] The large difference between the electrochemical performances of Li_2MnSiO_4 and Li_2FeSiO_4 is mainly attributed to the Jahn–Teller distortion associated with the Mn^{3+}, which causes a big change in the lattice parameters and destroys the crystalline structure of the material. Irreversible changes in the local environment of Mn ions on oxidation/reduction cycle of Li_2MnSiO_4 were revealed by in-situ X-ray absorption spectroscopy (XAS).[18] In order to improve the cycling stability of Li_2MnSiO_4 and the discharge capacity of Li_2FeSiO_4, partial substitution of Mn-site with Fe has been performed on $Li_2Fe_xMn_{1-x}SiO_4$ ($0 < x < 1$) to improve the electrochemical performance.[89,188,196,198] $Li_2Mn_xFe_{1-x}SiO_4$ solid solutions were formed within a wide compositional range with $0 < x < 1$.[196] An optimized capacity for $Li_2Mn_xFe_{1-x}SiO_4$ was achieved at $x = 0.5$, which shows a capacity of 235 mAh/g. DFT calculation results also confirmed that $Li_2Mn_xFe_{1-x}SiO_4$ might be more stable under reversible exchange of more than one Li (p.f.u.) by using an appropriate Mn/Fe mixture.[89] Although the electrochemical activity of Li_2MnSiO_4 can be improved through Mn-site substitution, the substitution of Mn-site with Fe was found to be unable to suppress the problematical distortion found in the Mn-coordination tetrahedron. Thus, finding an effective approach to stabilize the structure of Li_2MnSiO_4 to sustain more than one Li exchange remains an exciting challenge for the future.

The electrochemical performance of Li_2CoSiO_4 was found to be poor for all the polymorphs synthesized.[19,20] Fig. 6 shows cyclic voltammogram and voltage profiles for a Li_2CoSiO_4 sample prepared by a hydrothermal reaction, respectively. Li_2CoSiO_4 shows an oxidation peak at about 4.3 V and a reduction peak at 4.1 V with high irreversible capacity loss in the first cycle. The poor electrochemical result may contribute to the low conductivity and structure instability of Li_2CoSiO_4. The theoretical study suggested an extraction of the second lithium ion would occur at a higher voltage ($\sim$ 5.0 V).[13] The average lithium deinsertion voltage for the second lithium lies above the stability of the most used electrolytes for lithium batteries; hence

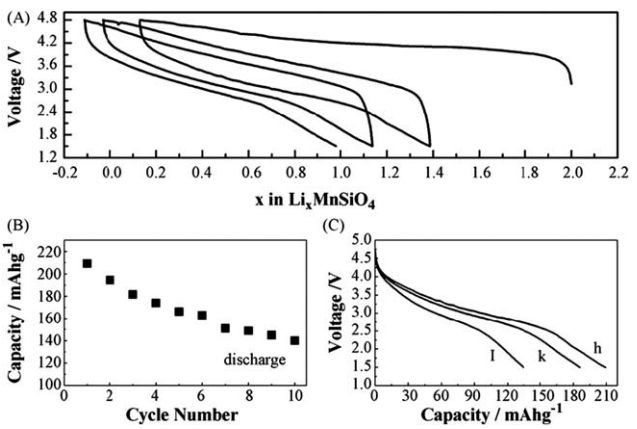

Fig. 5 Electrochemical performances of Li_2MnSiO_4/C nanocomposite material: (A) voltage *vs.* composition curves at 5 mA g^{-1}; (B) cycling performance between 1.5 and 4.8 V at 5 mA g^{-1}; (C) first discharge curves at different current densities: (h) 5 mA g^{-1}; (k) 30 mA g^{-1}; (l) 150 mA g^{-1} (from ref. 17.).

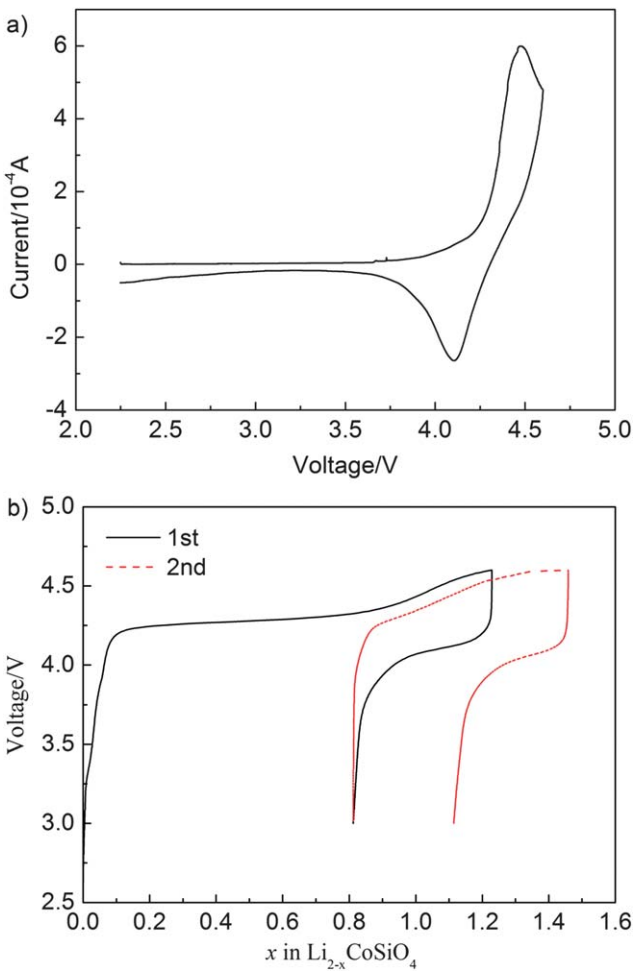

Fig. 6 (a) Cyclic voltammogram for a Li_2CoSiO_4 sample prepared by a hydrothermal reaction at 0.2 mV s^{-1} between 3.0 and 4.6V *vs.* Li/Li^+ in 1M $LiPF_6$/EC +DMC (1 : 1); (b) voltage profiles of Li_2CoSiO_4 sample prepared by a hydrothermal reaction cycled at a rate of 5 mA g^{-1} (from ref. 19.).

a more stable electrolyte (such as ionic liquids, *etc.*) that can sustain higher voltages is necessary in order to apply the second lithium of this compound.

Theoretical calculations were widely used to study the structure and electrochemical performance of Li_2MSiO_4 polymorphs.[13,85–87,89,182,198–200] The calculated lithium deinsertion voltages for all the studied orthosilicates are close to the experimental values.[13] Consistent with experimental results, the partially delithiated $LiFeSiO_4$ phase was found to be very stable.[86] Good reversibility upon the de-/intercalation process was predicted, and the possibility of reversible exchange of more than one electron was found to be hindered by the high stability of the intermediate phase $LiFeSiO_4$. However, the original host structure of Li_2MnSiO_4 was found to collapse upon being delithiated, with a strong tendency to amorphize.[89] The most favorable intrinsic defect type for Li_2MSiO_4 was found to be the mixing of the Li- and M-site occupation.[201] The exact concentration of Li/M mixing is correlated with polymorphs of Li_2MSiO_4 and depends on temperature, hence is sensitive to synthetic routes and thermal history. The Li- and Fe-site exchange were also observed in the process of electrochemical cycling. According to the density functional theory (DFT) study results, such mixing does not appear to impede the Li vacancy migration, it even opens alternative pathways for effective Li-migration in all three dimensions by the percolation of corner-sharing tetrahedral sites throughout the structure.[202] Atomistic simulation results suggest that curved Li diffusion paths and anisotropic nature of the Li transport in Li_2MnSiO_4 may be general for the Li_2MSiO_4 (M = Mn, Fe, Co) family of compounds.[201] The lowest active energies for Li migration in Li_2MSiO_4 polymorphs were found to be different. Such differences in intrinsic Li mobility would influence their electrochemical performance, especially the rate capability as rechargeable electrodes. The substitution of SiO_4^{4-} for VO_4^{3-} polyanions in Li_2FeSiO_4 was explored by the density functional theory (DFT), in order to enhance the electron transfer between the TM-ions and thereby to achieve a capacity increase from the potential redox activity of the orthovanadate polyanion.[203] Density functional theory (DFT) study results suggest that 12.5% substitution of VO_4^{3-} into the SiO_4^{4-} site in Li_2FeSiO_4 results in improved electronic transport and increased capacity.

As new polyanion-based cathode materials, orthosilicates, although promising, raise many scientific issues that need to be explored using combined experimental and theoretical approaches. However, special attention should be paid to the oxygen coordination polyhedral environments of transition metal ions in Li_2MSiO_4 and delithiated $Li_{2-x}MSiO_4$. As both Fe^{2+}, Fe^{3+} and even Fe^{4+} are found to be stable in tetrahedral coordination; it is not a surprise that Li_2FeSiO_4 possesses both high thermal and cycle stability. However, the poor cycle performance of Li_2MnSiO_4 and Li_2CoSiO_4 is perhaps caused by the instability of Mn^{4+} or Co^{4+} in tetrahedral oxygen coordination, as Mn^{4+} or Co^{4+} in tetrahedral coordination is rarely encountered and Mn^{3+} ions prefer the octahedral sites to the tetrahedral sites. An irreversible phase transformation in Li_2MnSiO_4 during delithiation can arise by the Mn ions rearranging their oxygen coordination upon oxidation. Thus, it could be very interesting and highly valuable to explore the Li_2MSiO_4 compounds with TM ions in octahedral oxygen coordination.

2.5 Fluorophosphates

Besides increasing the specific capacity of electrodes, increasing the cathode potential (*ca.* high operating cell voltage) would be another way to improve the energy density of today's lithium ion batteries. Fluorophosphates combine the inductive effect of the PO_4^{3-} group and the high electronegativity of the F^- anion, which show to be potential high voltage cathode materials.

Barker *et al.* first reported the lithium ion insertion/extraction behavior in the fluorophosphate phase, $LiVPO_4F$.[22,204–207] $LiVPO_4F$ is isostructural with the naturally-occurring mineral tavorite, $LiFePO_4 \cdot OH$,[208] crystallizing with a triclinic structure (space group $P\bar{1}$). $LiVPO_4F$ comprises a three-dimensional framework built up from PO_4 tetrahedra and an oxyfluoride sublattice. Li ions are statistically distributed on two (energetically inequivalent) crystallographic sites. The potential of de-/lithiated based on reversibility V^{3+}/V^{4+} is near 4.2 V *vs.* Li, around 0.3 V higher than that for the same transition in the lithium vanadium phosphate, $Li_3V_2(PO_4)_3$.[22] Electrochemical measurements reveal the extraction of Li ions from two crystallographic sites within the $LiVPO_4F$ framework in the first charge process, while the subsequent lithium insertion process proceeds *via* a two-phase reaction mechanism.[206] A capacity of 155 mAh/g close to the theoretical value (156 mAh/g) was obtained at a slow cycling rate through optimizing preparative conditions. Long-term cycling studies show that the total capacity loss is ~14% after 1260 cycles with an initial capacity of 122 mAh/g when cycled at 0.92 C.[24] A preliminary test showed that $LiVPO_4F$ also possesses excellent thermal stability.[25]

Barker *et al.* further demonstrated the feasibility of directly using sodium-based compounds ($NaVPO_4F$) as cathode materials for lithium ion batteries without prior ion exchange (Na → Li).[23,209] Followed by $NaVPO_4F$, another sodium-based fluorophosphates phase $Na_3V_2(PO_4)_2F_3$ was explored as cathode material by Barker *et al.*[26,210] The theoretical capacity for $Na_3V_2(PO_4)_2F_3$ is 192 mAh/g assuming that all three sodium ions may be reversibly cycled. From the initial measurements, a practical capacity of around 120 mAh/g at an average potential of 4.1 V *vs.* Li was acquired. The extraction of the third Na^+ ion from $Na_3V_2(PO_4)_2F_3$ is found to be accompanied by some concurrent structural degradation. For an electrochemical test, metallic lithium or graphite anode and lithium salt electrolyte were used. Sodium is deintercalated from the positive electrode upon the initial charge, resulting in a mixed alkali electrolyte composition. Sodium and lithium are believed to co-intercalate on discharge. Intriguingly, the presence of Na^+ in the electrolyte showed no negative effects on the long-term performance characteristics of the cell, demonstrating the reversible cyclability of sodium based cathode materials in lithium ion cells. This development opened up a field to the direct use of sodium cathode materials in lithium ion batteries, especially for these materials whose lithium based phase can't be synthesized directly, without the requirement for ion exchange (Na, K → Li) prior to cell assemblage.

The structure and electrochemical performance of $Li_5V(PO_4)_2F_2$ as a 4 V class cathode material were studied by Nazar and co-workers.[28,29] $Li_5V(PO_4)_2F_2$ has a two dimensional layered monoclinic structure which consists of alternately stacked vanadium fluorophosphates and lithium slabs. The theoretical

capacity based on $V^{3+}/V^{4+}/V^{5+}$ redox couples is 170 mAh/g. Two plateaus at 4.15 and 4.65 V corresponding to V^{3+}/V^{4+} and V^{4+}/V^{5+} redox couples were observed during the first charge process. However, it was found that only the V^{3+}/V^{4+} redox couple is lithium extraction/insertion reversible, the second process at 4.65 V shows poor reversibility.

Besides vanadium, other transition metal fluorophosphate phases A_2MPO_4F (A = Li, Na; M = Co, Ni, Fe, Mn)[30–34,37,211] were also recently explored as cathode materials. A_2MPO_4F crystallize in three different structures due to the subtle effects of ion size mediated interactions and magnetic interactions.[34] The structures of layered Na_2FePO_4F and Na_2CoPO_4F, the "stacked" Li_2CoPO_4F and Li_2NiPO_4F, and the 3D Na_2MnPO_4F are greatly different (Fig. 7). The transition metal locates in octahedral sites for all three, however, the connectivity of the octahedra varies from mixed face-shared and corner-shared in the layered structure to edge-shared in the "stacked" structure and corner-shared in the 3D structure. Na_2MPO_4F (M = Co, Ni, Fe) and their lithium phase were all found to be electrochemically reversible, however, Na_2MnPO_4F was found to be electrochemically irreversible despite an open pathway for alkali migration. Whether this is due to the structural distinction of Na_2MnPO_4F is not clear at present.

The structure and electrochemical properties of A_2FePO_4F (A = Li, Na) were studied in detail by Nazar and Tarascon *et al.* recently.[31–34] Na_2FePO_4F crystallizes with an orthorhombic structure (space group *Pbcn*). The structural features of Na_2FePO_4F that include pairs of face-sharing metal octahedra and [6 + 1] coordination of the sodium ions were confirmed by single crystal X-ray diffraction. Na_2FePO_4F possesses two-dimensional ion transport paths, which facilitates the ionic conductivity. It exhibits a staircase voltage profile spanning the single phase $Na_{1.5}FePO_4F$ with lattice parameters intermediate between the two end members. Differing from $LiFePO_4$, a sloping voltage profile was observed for Na_2FePO_4F and indicating a quasi-solid solution electrochemical behavior. The unit-cell volume change from Na_2FePO_4F to an oxidized compound (Na_2FePO_4F) is only 4%, and thus a lower-strain de-/intercalation process is expected. Na_2FePO_4F shows an average potential of 3.5 V on cycling which is comparable to that of $LiFePO_4$ (3.55 V). A reversible capacity of 115 mAh/g (85% of the theoretical capacity) was obtained on the first cycling and good cycling stability was observed. $LiFePO_4F$ prepared by the solid state route and ionothermal reaction is isostuctural with the mineral tavorite with space group $P\bar{1}$. A reversible capacity of 145 mAh/g corresponding to 0.96 Li exchange was obtained with an overall potential around 3 V cycling between $LiFePO_4F$ and Li_2FePO_4F. Surprisingly, the oxidation of Fe^{3+} to Fe^{4+} *via* electrochemical oxidization of $LiFePO_4F$, although limited ($\Delta x \approx 0.1$), was proved to be feasible.[31] The appearance of structural phase changes for each staircase voltage change was investigated by *in situ* XRD and Mössbauer measurements.

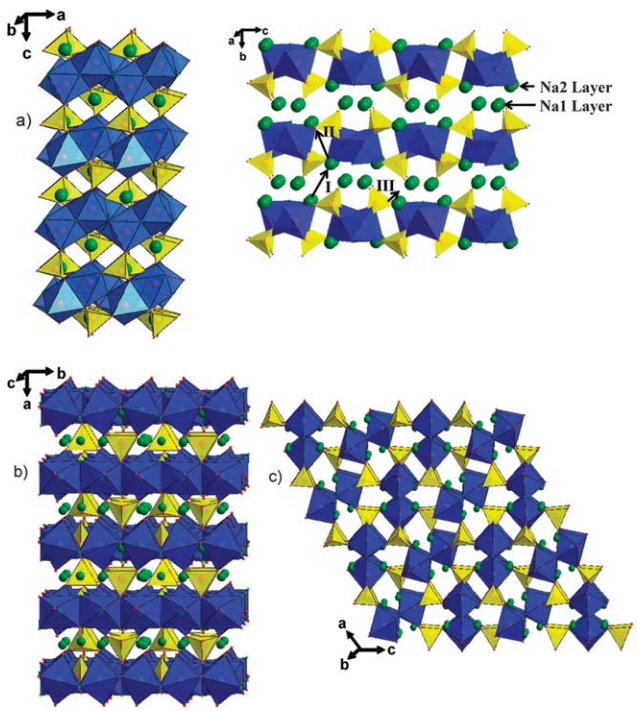

Fig. 7 Crystal structure of Na_2FePO_4F (layered): (a) view along [010] and [100]. Ion transport pathways (I, II, and III) are marked. (b) The crystal structure of Li_2CoPO_4F (stacked) and (c) the structure of Na_2MnPO_4F (3D). The transition metal octahedra are shown in blue, phosphate tetrahedra in yellow, and alkali ions in green (from ref. 34.).

Li_2CoPO_4F[35] and Li_2NiPO_4F[37] were proposed as potential cathode materials with both large capacity and high discharge voltage. Li_2CoPO_4F exhibits a higher 5.0 V discharge plateau with a practical capacity of 120 mAh/g.[36] According to GGA + U calculation by Ceder *et al.*, the redox potential of $LiNiPO_4$ is 5.1V *versus* Li/Li^+, we can conclude that the redox potential of Li_2NiPO_4F would be above the electrolytic stability window of most electrolytes. For this reason, the cathode properties of Li_2NiPO_4F were not reported until Masatoshi *et al.*[37] proved recently that Li_2NiPO_4F has actually *ca.* 5.3 V redox potential *versus* Li/Li^+ using a sebaconitrile-based oxidation resistant electrolyte. The theoretical capacity of Li_2CoPO_4F and Li_2NiPO_4F reached about 310 mAh/g based on two lithium reactions, which is almost twice as large as that of $LiMPO_4$. Unfortunately, their true capacity and cyclability are still unknown because of electrolyte instability. Importantly, it was also found that delithiated Li_2CoPO_4F exhibited good thermal stability due to the less amount of Co^{4+} in charged $Li_{2-x}CoPO_4F$.[36]

When lithium ion batteries were used in PHEV/EV, safety is a critical consideration, as the risks increase with the energy stored in batteries. To eliminate the safety problems raised by the highly reactive lithiated graphite and the formation of solid electrolyte interface (SEI) layer at the carbon negative electrode, less reducing materials (such as $Li_4Ti_5O_{12}$, Ti_2O, *etc.*) were proposed as anode material to replace carbon.[212–214] However, this approach seriously decreases the operating voltage of the resulting batteries and, consequently the energy density of batteries. Such $Li_4Ti_5O_{12}$ || $LiFePO_4$ configuration cell operates at an average discharge voltage of around 1.8 V.[213,214] The development of high voltage cathode materials may provide an opportunity to address this shortcoming by combining the high electrode potential of fluorophosphates and the high safety of Ti-based anodes. Furthermore, increasing the positive electrode voltage (5 V or higher) would be a promising approach to improve the energy density of lithium ion cells. However, the development of positive electrodes based on higher potential

insertion materials was constrained by the relatively narrow stability window (lower than 5 V) of the current organic electrolytes. If this can be solved *via* the development of the next generation of electrolytes with high-voltage stability window, the batteries of the future would be smaller and lighter (*ca.* with higher specific energy density) *via* the use of high voltage cathode materials, such as fluorophosphates, *etc*.

It should be mentioned that the detailed function mechanism of the introduced F-ions to the properties of fluorophosphates is not well understood at the present time, although the electrochemical properties of some fluorophosphate-type compounds have been investigated. It is highly desirable that some fundamental understanding both experimental and theoretical of the effects of the introduced F- on the structure feature, electrochemical properties (such as redox potential, electronic and ionic conductivity) of fluorophosphates, and also whether more than one lithium p.f.u. can be reversibly extracted from fluorophosphate compounds and how to realize it experimentally.

2.6 Fluorosulphates

$LiMSO_4F$ as novel cathode materials were first reported by Tarascon and co-workers in 2010.[38] As showed by Padhi *et al.*, the substitution of $(PO_4)^{3-}$ by $(SO_4)^{2-}$ in an isostructural NASICON $Li_xM_3(XO_4)_3$ host can lead to an increase in the redox potential by 0.8 V due to the inductive effect. Considering this, lithium metal sulphates would be another group of attractive cathode materials. However, sulphates encounter the problem of low negative charge of the $(SO_4)^{2-}$ unit, which requires the addition of a charged anion for charge balance to afford reversible electron exchange. Fluoride would be an available choice, as F^- is the lightest and most electronegative singly charge anion and the feasibility of combining fluoride and phosphates has already been reported. In 2002, Sebastian *et al.*[215] reported that a lithium fluorosulphate phase $LiMgSO_4F$ exhibits significant Li-ion conduction. According to their results the authors conclude that 'Li-ion conduction in $LiMgSO_4F$ suggests that isostructural metal analogues $LiMSO_4F$ (M = Mn, Fe, Co) would be important for redox extraction/insertion of lithium involving M^{II}/M^{III} oxidation states'. However, the electrode properties of fluorosulphates had not been investigated, until Tarascon and co-workers reported recently $LiFeSO_4F$ as a novel 3.6 V cathode material with promising electrochemical performance.[38] Based on the results of their work, this is mainly attributed to the instability of $LiMSO_4F$ (M = Mn, Fe, Co) at high temperatures (500–900 °C) of normal solid state reactions. The large solubility of the sulphates and instability of $LiFeSO_4F$ in water made aqueous routes also precluded.

Using ionothermal synthesis, Tarascon and co-workers successfully presented $LiFeSO_4F$ with a tavorite-type structure as an attractive 3.6 V cathode candidate with a theoretical capacity of 151 mAh/g.[38] The crystal structure (Fig. 1e and 1f) of $LiFeSO_4F$ is isotypic with triclinic $LiMgSO_4F$[215] with a space group $P\bar{1}$, which is built from two crystallographically distinct and slightly distorted FeO_4F_2 octahedra and SO_4 tetrahedra. Each FeO_4F_2 octahedron shares two corners (F^- ions) with adjacent octahedra to form chains running along the *c*-axis. The isolated SO_4 tetrahedra cross-link three chains *via* corner sharing with four different octahedra. Within this framework, Li^+ ions reside in three cavities forming tunnels delimited by the framework along the [100], [010] and [101] directions (Fig. 8). Thermal gravimetric analysis (TGA) coupled with mass spectrometry analysis confirm the thermodynamically instability of $LiFeSO_4F$ and the onset of sample decomposition occurring near 350 °C. Good electrochemical performance can be obtained for $LiFeSO_4F$ without the need for carbon coating and/or resorting nanoparticles. It delivers a reversible capacity of about 130 to 140 mAh/g centered around 3.6 V *vs.* Li at C/10 rate with excellent capacity retention (Fig. 9). 85% of the total electrode initial capacity can be delivered at 1 C rate suggesting that $LiFeSO_4F$ could sustain reasonable rate capabilities. *In situ* XRD measurements indicated a two-phase reaction mechanism in agreement with the flat charge-discharge profile. Primary conductivity measurements showed that the electronic conductivities for $LiFeSO_4F$ and $LiFePO_4$ are in the same range of magnitude, whereas the ionic conductivity of $LiFeSO_4F$ is much higher than that of $LiFePO_4$ ($\approx 4 \times 10^{-6}$ S cm^{-1} for $LiFeSO_4F$ *vs.* 2×10^{-9} S for $LiFePO_4$ at 147 °C). The higher ionic conductivity of $LiFeSO_4F$ would improve its packing density *via* avoiding the necessitating nanosizing and/or carbon coating. Considering the highly costly ionic liquids, the authors declared that 'the ionic liquids can be easily recovered and recycled'. However, although ionic liquids can be recovered and further used for subsequent synthesis, they are inherently expensive. To account for this, a novel solid-state process was developed recently by Tarascon and co-works for preparing $LiFeSO_4F$ at the expense of both longer reaction time and slightly contaminated samples as compared to the ionothermal process. The resulting material exhibits an electrochemical performance comparable with those obtained by an ionothermal process. This

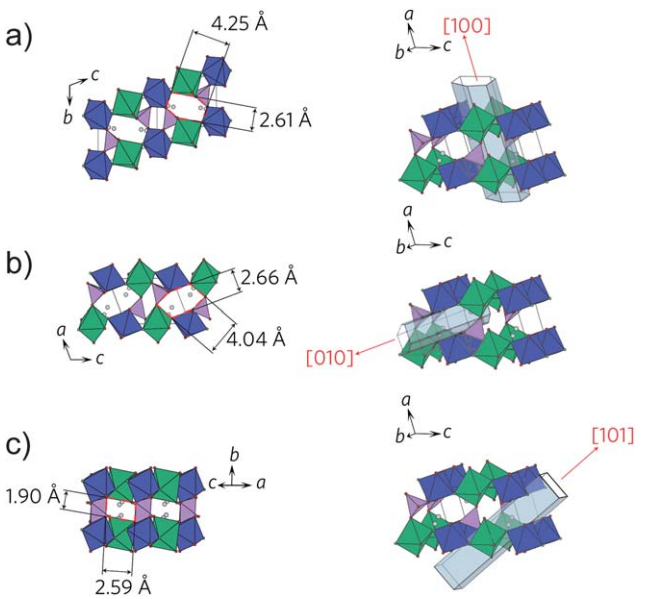

Fig. 8 Projections of the $LiFeSO_4F$ structure along the [100] (a), [010] (b) and [101] (c) directions, with the tunnels along those three directions for possible ion migrations highlighted together with the tunnel distances. MO_4F_2 octahedra are represented in blue and green and SO_4 tetrahedra are in purple (from ref. 38.).

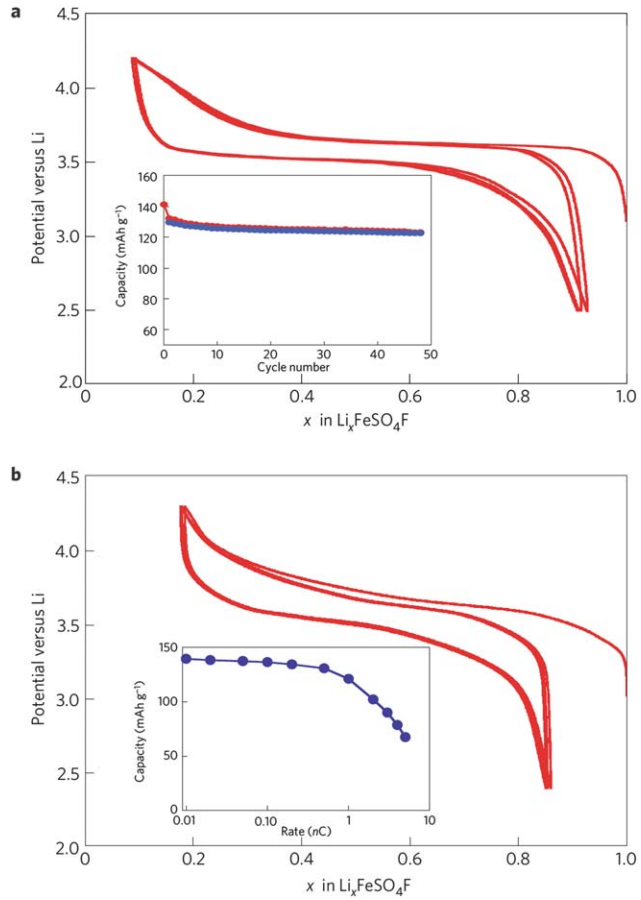

Fig. 9 Electrochemical characterizations of $LiFeSO_4F$ powders. Charge/discharge galvanostatic curves for Li/$LiFeSO_4F$ cells cycled between 2.5 and 4.2 V at C/10 (1 Li in 10 h) (a) and C/2 (1 Li in 2 h) (b), highlighting the sustained reversible capacity of the electrode and the near 100% cycling capacity efficiency. Electrodes were made by ball-milling for 15 min and 30 min $LiFeSO_4F$ (85%)/carbon (15%) mixtures for the cells in a and b, respectively. The capacity retention of such cells (red for charge and blue for discharge) together with their power rate (discharge capacity is plotted as a function of the rate n C) are shown as insets in a and b, respectively. Within such measurements, currents of 1.2 mAcm^{-2} were used for the 1 C rate (from ref. 38.).

suggests economic scale-up novel synthesis approaches should be developed for fluorosulphate cathodes.

Following on from their first work on $LiFeSO_4F$, Tarascon and co-workers further explored the structure and electrochemical properties of other isostructural $AMSO_4F$ (A = Na, Li; M = Fe, Co, Ni, Mn)[39] phases and $(Na_{1-x}Li_x)(Fe_{1-x}M_x)SO_4F$ (M = Fe, Co, Ni)[40] solid-solution phases prepared by both ionothermal and solid-state synthesis. The crystal structures of $LiCoSO_4F$ and $LiNiSO_4F$ were similar to $LiFeSO_4F$ and can be indexed to a triclinic unit cell with space group $P\bar{1}$. Interestingly, $LiMnSO_4F$ was found to crystallize in a monoclinic system, space group $P2_1/c$, and shows the highest thermal stability without decomposition up to 600 °C in air. The thermal stability of fluorosulphates was positively correlated to the ionic radii of M cations, falls in the order of $LiNiSO_4F$ (350 °C) < $LiCoSO_4F$ (375 °C) < $LiFeSO_4F$ (400 °C) < $LiMnSO_4F$ (600 °C). For Li$(Fe_{1-x}M_x)SO_4F$ solid solution phases, only the 3.6 V $Fe^{2+/3+}$ redox reaction is observed with no signature of $Co^{2+/3+}$, $Ni^{2+/3+}$ or $Mn^{2+/3+}$ reaction. $LiMSO_4F$ (M = Co, Ni, Mn) phases were found to be electrochemically inactive by cycling up to 5 V, which implies most likely that the potential of M^{2+}/M^{3+} redox couples lies above 5.0 V.

The success development of $LiFeSO_4F$ as cathode material suggests more polyanion compounds can be explored as novel insertion materials for lithium batteries.

2.7 Borates

Although polyanions shows a lot of advantages as cathode materials for lithium ion batteries, the polyanion groups also bring some inactive mass into the electrode resulting in relatively low theoretical capacity of polyanion compounds (such as 170 mAh/g for $LiFePO_4$), which lowers both the specific capacity and the specific energy. Considering this, the development of borate compounds as cathode materials would be very attractive, as the $(BO_3)^{3-}$ unit is the lightest polyanion group. In the early 2000s, researchers started to evaluate the potential of borates as cathode materials,[42] however impressive electrochemical performance was only achieved recently by Yamada's group.[41]

In 2001, Legagneur *et al.*[42] explored the structure and cathode performance of $LiMBO_3$ (M = Mn, Fe, Co) synthesized by a solid state reaction as new cathode materials. The crystal structures of $LiMBO_3$ were determined from single crystal data. $LiFeBO_3$ and $LiCoBO_3$ exhibit the same structure (Fig. 1g and 1h). The three-dimensional $[FeBO_3]_n^{n-}$ framework is built up from edge sharing FeO_5 trigonal bipyramids and BO_3 groups, within the distorted hexagonal closed-packed (hcp) oxygen subarray. Each FeO_5 bipyramid (iron statistically occupies two trigonal sites) shares two edges with adjacent bipyramids to form single chains running along the [-101] direction. The planar BO_3 groups link three chains *via* corner sharing. Within this framework, edge-sharing chains of paired face-sharing LiO_4 tetraheda (lithium statistically occupies two tetrahedral sites) align in parallel chains along the [001] direction. The structure of *h*-$LiMnBO_3$ is isotypic with the hexagonal form of $LiCdBO_3$. For all of the three borates, the results showed very limited electrochemical activity, the reversible exchange of lithium was limited to 0.04 Li per formula unit. However, an important inductive effect of the BO_3 group was demonstrated from the thermodynamic study performed for $LiFeBO_3$, which showed the Fe^{3+}/Fe^{2+} reduction couple lies between 3.1 V/Li and 2.9 V/Li.

Since then, very few works have been reported on this type of materials for cathode applications, and all showed unimpressive electrochemical performance, with very small capacity and/or very large polarization without any visible plateau-like voltage region, including some conversion-type reduction to Fe metal occurring at potentials below 2 V.[216–218] A major breakthrough was made by Yamada's group recently,[41] a very carefully prepared (keeping the samples in an inert atmosphere after synthesis to avoid poisoning by air exposure) $LiFeBO_3$ material with good cathode performance was reported. The obtained material exhibits a larger reversible capacity of *ca.* 200 mAh/g at around 3 V *versus* lithium. After optimization, 80% of the initial capacity can be retained even at the high rate of 2 C, with negligible cycle degradation. Both experiments and *ab initio* calculations confirmed solid-solution behavior between

isostructural end members with a very small volume change (*ca.* 2%) suitable for a reversible reaction. From *ab initio* calculation results, surface poisoning is expected for $LiFeBO_3$, as the potential for stoichiometric $LiFeBO_3$ was estimated to be lower than 2.6 V, which is sufficiently low to function as a reducing agent for moisture. A significant improvement in electrochemical performance was achieved by avoiding surface poisoning due to contact with the ambient atmosphere. These indicate that borates with the lightest polyanion group could be potential cathode candidates for advanced lithium batteries. However, surface poisoning due to contact with the ambient atmosphere is an important factor needing to be investigated and solved before their application in commercial products can be considered.

2.8 Other polyanion compounds

Apart from the above-mentioned polyanion compounds which are already studied widely, other polyanion compounds such as $LiMXO_4$, (M is transition metal, X = As, Mo, W, *etc.*) have also been explored as cathode materials for lithium ion batteries in recent years. However, the theoretical capacity of arsenates is somewhat lower than the widely studied phosphate compounds, due to the higher molecular weight of the arsenate group. For molybdates and tungstates, it is hoped to improve the specific capacity *via* involving the Mo^{6+}/Mo^{x+} and W^{6+}/W^{x+} ($x = 4$ or 5) redox couple. However, the Mo^{6+}/Mo^{x+} redox couple was found to be irreversible in most cases, perhaps due to the instability of tetrahedrally coordinated Mo^{5+} or Mo^{4+} ions.[219] Arroyo-de Dompablo *et al.*[220,221] investigated the electrochemical performance of olivine-$LiCoAsO_4$ experimentally and computationally. Both experimental and computational results show $LiCoAsO_4$ is electrochemically active with an average insertion voltage of 4.7 V, which is slightly lower (about 0.1 V) than its phosphate analogues $LiCoPO_4$, due to the slightly less covalent nature of the AsO_4^{3-} group. The general electrochemical characteristics of $LiCoAsO_4$ and $LiCoPO_4$ are similar. At the first cycle, about 0.78 Li^+ per formula unit (p.f.u) was extracted from $LiCoAsO_4$ on charge and 0.45 Li^+ p.f.u can be reinserted in following discharge process. At the same time, Satya Kishore *et al.*[222] studied the electrochemical performance of olivine-$LiCoAsO_4$ prepared by a solid state reaction and got similar results. Began *et al.* explored the electrochemical properties of polyanion-type $Li_2M_2(MoO_4)_3$ (M = Ni, Co, Mn) as cathode materials in lithium ion batteries.[219,223–226] Their results showed that these materials did not demonstrate any useful electrochemical properties as cathode materials for lithium ion batteries, although they possess an open framework NASICON type structure. All the studied materials showed very poor cycle stability due to the drastic structural changes accompanied by exponential capacity decay. After optimization by adding nano-sized carbon as a conductive additive, $Li_2Co_2(MoO_4)_3$ exhibited an initial discharge capacity of 121 mAh/g with 55% retention after 20 cycles between 3.5–2 V.[227] For $Co_2(MoO_4)_3$, more than 2 Li p.f.u. can be inserted, corresponding to the Co^{3+}/Co^{2+} redox couple located at 2.6 V, and the irreversible Mo^{6+}/Mo^{5+} redox couple located at 2.2 V, respectively.[219] Lithium intercalation into $Li_3Fe(MoO_4)_3$ was found to occur at 2.4 V with the formation of $Li_4Fe(MO_4)_3$.[228,229] Recently, Mikhailova *et al.*[230] investigated both the Li extraction and insertion behavior of orthorhombic NASICON-$Li_3V(MoO_4)_3$. Lithium extraction from $Li_3V(MoO_4)_3$ occurs at 3.7 V with the formation of $Li_2V(MoO_4)_3$ and preserving the space-group symmetry. Also, reversible Li insertion into $Li_3V(MoO_4)_3$ occurs at 2.1 V with the formation of isostructural $Li_4V(MoO_4)_3$. The oxidation of $Li_3V(MoO_4)_3$ was found to be associated with V^{3+}/V^{4+} redox couple, whereas the reversible reduction of $Li_3V(MoO_4)_3$ is associated mainly with the Mo^{6+}/Mo^{5+} redox couple, and partly with the V^{3+}/V^{2+} redox couple. Li *et al.*[231,232] studied the electrochemical properties of a tungstate thin film fabricated by radio-frequency (R.F.) sputtering deposition as the cathode. Two redox couples, Fe^{3+}/Fe^{2+} and W^{6+}/W^{x+} ($x = 4$ or 5), were found to be electrochemical active for $LiFe(WO_4)_2$, corresponding to two plateaus at 3 V and 1.5 V regions, respectively.

3. Summary and outlook

The rapid development of Li-ion batteries impacts on a strong requirement for safe and high energy density electrode materials, especially for cathode materials. Successful application of $LiFePO_4$ in high-power batteries has stimulated big interest in the search for a new class of polyanion compounds as the next generation electrode materials for Li-ion batteries. It is clearly seen that polyanion compounds do provide a new class of electrode materials with the possibility to design their composition and structure. The stable framework of the polyanion compounds provide feasibility for hosting more than one-electron exchange reaction per formula unit. Therefore, they have an instinctive high capacity and thermal stability character. However, we are still in the early stages to develop polyanion compounds as matured electrode materials for practical batteries. There is a big opportunity to explore this exciting field in the future. The challenges may include: How to design and keep the polyanion framework stable under multiple-electron exchange process? Is it possible to summarize some general principles for designing and constructing polyanion electrode materials? What's the space limit for developing such kind of compounds? We believe that a new system (incl. new polyanion or polyanion-combination framework of phosphate and sulfate, borates or silicates), a new synthesis method and an electrochemical reaction mechanism study of the new materials should be stressed in the following research activity. Since the intrinsic low electronic conductivity of polyanion compounds, the development of polyanion/graphene composite will be a good way for the synthesis of high-performance polyanion-based electrode materials. Future work should be explored and combined by the contribution from different fields: *i.e.* inorganic chemists, material scientists, electrochemists, *etc.* As an optimistic view, we believe that we would find some way to solve those challenging problems in the near future.

Acknowledgements

We are grateful to the sponsors of the research in our group in the last decades: the National Natural Science Foundation of China (Grant No. 20873115, 21021002 and 90606015, *etc.*), and the National Basic Research Program of China (973 program, Grant No. 2007CB209702, 2011CB935903).

References

1 J. M. Tarascon and M. Armand, *Nature*, 2001, **414**, 359–367.
2 J. M. Tarascon, *Philos. Trans. R. Soc. London, Ser. A*, 2010, **368**, 3227–3241.
3 A. K. Padhi, K. S. Nanjundaswamy and J. B. Goodenough, *J. Electrochem. Soc.*, 1997, **144**, 1188–1194.
4 A. S. Andersson, J. O. Thomas, B. Kalska and L. Haggstrom, *Electrochem. Solid-State Lett.*, 1999, **3**, 66–68.
5 G. H. Li, H. Azuma and M. Tohda, *Electrochem. Solid-State Lett.*, 2002, **5**, A135–A137.
6 G. Y. Chen and T. J. Richardson, *J. Power Sources*, 2010, **195**, 1221–1224.
7 S. M. Oh, S. W. Oh, C. S. Yoon, B. Scrosati, K. Amine and Y. K. Sun, *Adv. Funct. Mater.*, 2010, **20**, 3260–3265.
8 K. Amine, H. Yasuda and M. Yamachi, *Electrochem. Solid-State Lett.*, 1999, **3**, 178–179.
9 H. H. Li, J. Jin, J. P. Wei, Z. Zhou and J. Yan, *Electrochem. Commun.*, 2009, **11**, 95–98.
10 F. Zhou, M. Cococcioni, K. Kang and G. Ceder, *Electrochem. Commun.*, 2004, **6**, 1144–1148.
11 J. Wolfenstine and J. Allen, *J. Power Sources*, 2005, **142**, 389–390.
12 A. Nyten, A. Abouimrane, M. Armand, T. Gustafsson and J. O. Thomas, *Electrochem. Commun.*, 2005, **7**, 156–160.
13 M. E. Arroyo-de Dompablo, M. Armand, J. M. Tarascon and U. Amador, *Electrochem. Commun.*, 2006, **8**, 1292–1298.
14 Z. L. Gong, Y. X. Li, G. N. He, J. Li and Y. Yang, *Electrochem. Solid-State Lett.*, 2008, **11**, A60–A63.
15 T. Muraliganth, K. R. Stroukoff and A. Manthiram, *Chem. Mater.*, 2010, **22**, 5754–5761.
16 R. Dominko, M. Bele, M. Gaberscek, A. Meden, M. Remskar and J. Jamnik, *Electrochem. Commun.*, 2006, **8**, 217–222.
17 Y. X. Li, Z. L. Gong and Y. Yang, *J. Power Sources*, 2007, **174**, 528–532.
18 R. Dominko, I. Arcon, A. Kodre, D. Hanzel and M. Gaberscek, *J. Power Sources*, 2009, **189**, 51–58.
19 Z. L. Gong, Y. X. Li and Y. Yang, *J. Power Sources*, 2007, **174**, 524–527.
20 C. Lyness, B. Delobel, A. R. Armstrong and P. G. Bruce, *Chem. Commun.*, 2007, 4890–4892.
21 A. R. West and F. P. Glasser, *J. Solid State Chem.*, 1972, **4**, 20–28.
22 J. Barker, M. Y. Saidi and J. L. Swoyer, *J. Electrochem. Soc.*, 2003, **150**, A1394–A1398.
23 J. Barker, M. Y. Saidi and J. L. Swoyer, *J. Electrochem. Soc.*, 2004, **151**, A1670–A1677.
24 M. V. Reddy, G. V. S. Rao and B. V. R. Chowdari, *J. Power Sources*, 2010, **195**, 5768–5774.
25 F. Zhou, X. M. Zhao and J. R. Dahn, *Electrochem. Commun.*, 2009, **11**, 589–591.
26 J. Barker, R. K. B. Gover, P. Burns and A. J. Bryan, *Electrochem. Solid-State Lett.*, 2006, **9**, A190–A192.
27 R. K. B. Gover, A. Bryan, P. Burns and J. Barker, *Solid State Ionics*, 2006, **177**, 1495–1500.
28 Y. Makimura, L. S. Cahill, Y. Iriyama, G. R. Goward and L. F. Nazar, *Chem. Mater.*, 2008, **20**, 4240–4248.
29 S. C. Yin, P. S. Herle, A. Higgins, N. J. Taylor, Y. Makimura and L. F. Nazar, *Chem. Mater.*, 2006, **18**, 1745–1752.
30 B. L. Ellis, W. R. M. Makahnouk, Y. Makimura, K. Toghill and L. F. Nazar, *Nat. Mater.*, 2007, **6**, 749–753.
31 N. Recham, J. N. Chotard, J. C. Jumas, L. Laffont, M. Armand and J. M. Tarascon, *Chem. Mater.*, 2010, **22**, 1142–1148.
32 T. N. Ramesh, K. T. Lee, B. L. Ellis and L. F. Nazar, *Electrochem. Solid-State Lett.*, 2010, **13**, A43–A47.
33 N. Recham, J. N. Chotard, L. Dupont, K. Djellab, M. Armand and J. M. Tarascon, *J. Electrochem. Soc.*, 2009, **156**, A993–A999.
34 B. L. Ellis, W. R. M. Makahnouk, W. N. Rowan-Weetaluktuk, D. H. Ryan and L. F. Nazar, *Chem. Mater.*, 2010, **22**, 1059–1070.
35 S. Okada, M. Ueno, Y. Uebou and J. Yamaki, *J. Power Sources*, 2005, **146**, 565–569.
36 S. Okada, M. Ueno, Y. Uebou, J. Yamaki and Ieice, Structure and cathode properties of $LiCOPO_4$ and Li_2CoPO_4F for high-voltage Li-ion batteries, *Denshi Joho Tsushin Gakkai Kikai Shinko Kaikan, Tokyo 105*, 2003.
37 M. Nagahama, N. Hasegawa and S. Okada, *J. Electrochem. Soc.*, 2010, **157**, A748–A752.
38 N. Recham, J. N. Chotard, L. Dupont, C. Delacourt, W. Walker, M. Armand and J. M. Tarascon, *Nat. Mater.*, 2009, **9**, 68–74.
39 P. Barpanda, N. Recham, J. N. Chotard, K. Djellab, W. Walker, M. Armand and J. M. Tarascon, *J. Mater. Chem.*, 2010, **20**, 1659–1668.
40 P. Barpanda, J. N. Chotard, N. Recham, C. Delacourt, M. Ati, L. Dupont, M. Armand and J. M. Tarascon, *Inorg. Chem.*, 2010, **49**, 7401–7413.
41 A. Yamada, N. Iwane, Y. Harada, S. Nishimura, Y. Koyama and I. Tanaka, *Adv. Mater.*, 2010, **22**, 3583.
42 V. Legagneur, Y. An, A. Mosbah, R. Portal, A. L. La Salle, A. Verbaere, D. Guyomard and Y. Piffard, *Solid State Ionics*, 2001, **139**, 37–46.
43 A. Yamada, S. C. Chung and K. Hinokuma, *J. Electrochem. Soc.*, 2001, **148**, A224–A229.
44 G. T. K. Fey and T. L. Lu, *J. Power Sources*, 2008, **178**, 807–814.
45 N. Iltchev, Y. K. Chen, S. Okada and J. Yamaki, *J. Power Sources*, 2003, **119–121**, 749–754.
46 K. F. Hsu, S. Y. Tsay and B. J. Hwang, *J. Mater. Chem.*, 2004, **14**, 2690–2695.
47 G. Arnold, J. Garche, R. Hemmer, S. Strobele, C. Vogler and A. Wohlfahrt-Mehrens, *J. Power Sources*, 2003, **119–121**, 247–251.
48 K. S. Park, J. T. Son, H. T. Chung, S. J. Kim, C. H. Lee and H. G. Kim, *Electrochem. Commun.*, 2003, **5**, 839–842.
49 S. F. Yang, P. Y. Zavalij and M. S. Whittingham, *Electrochem. Commun.*, 2001, **3**, 505–508.
50 S. F. Yang, Y. N. Song, P. Y. Zavalij and M. S. Whittingham, *Electrochem. Commun.*, 2002, **4**, 239–244.
51 S. Ferrari, R. L. Lavall, D. Capsoni, E. Quartarone, A. Magistris, P. Mustarelli and P. Canton, *J. Phys. Chem. C*, 2010, **114**, 12598–12603.
52 A. V. Murugan, T. Muraliganth and A. Manthiram, *Electrochem. Commun.*, 2008, **10**, 903–906.
53 A. V. Murugan, T. Muraliganth and A. Manthiram, *J. Phys. Chem. C*, 2008, **112**, 14665–14671.
54 S. L. Yang, X. F. Zhou, J. G. Zhang and Z. P. Liu, *J. Mater. Chem.*, 2010, **20**, 8086–8091.
55 N. Recham, L. Dupont, M. Courty, K. Djellab, D. Larcher, M. Armand and J. M. Tarascon, *Chem. Mater.*, 2009, **21**, 1096–1107.
56 J. M. Tarascon, N. Recham, M. Armand, J. N. Chotard, P. Barpanda, W. Walker and L. Dupont, *Chem. Mater.*, 2010, **22**, 724–739.
57 M. Takahashi, S. Tobishima, K. Takei and Y. Sakurai, *J. Power Sources*, 2001, **97–98**, 508–511.
58 S. Franger, F. Le Cras, C. Bourbon and H. Rouault, *J. Power Sources*, 2003, **119–121**, 252–257.
59 N. Ravet, Y. Chouinard, J. F. Magnan, S. Besner, M. Gauthier and M. Armand, *J. Power Sources*, 2001, **97–98**, 503–507.
60 H. Huang, S. C. Yin and L. F. Nazar, *Electrochem. Solid-State Lett.*, 2001, **4**, A170–A172.
61 Y. G. Wang, Y. R. Wang, E. J. Hosono, K. X. Wang and H. S. Zhou, *Angew. Chem., Int. Ed.*, 2008, **47**, 7461–7465.
62 M. Koltypin, D. Aurbach, L. Nazar and B. Ellis, *J. Power Sources*, 2007, **174**, 1241–1250.
63 R. Dominko, M. Bele, M. Gaberscek, M. Remskar, D. Hanzel, J. M. Goupil, S. Pejovnik and J. Jamnik, *J. Power Sources*, 2006, **153**, 274–280.
64 J. S. Yang and J. J. Xu, *Electrochem. Solid-State Lett.*, 2004, **7**, A515–A518.
65 J. K. Kim, J. W. Choi, G. S. Chauhan, J. H. Ahn, G. C. Hwang, J. B. Choi and H. J. Ahn, *Electrochim. Acta*, 2008, **53**, 8258–8264.
66 J. J. Chen and M. S. Whittingham, *Electrochem. Commun.*, 2006, **8**, 855–858.
67 J. Chen, S. Wang and M. S. Whittingham, *J. Power Sources*, 2007, **174**, 442–448.
68 K. Shiraishi, K. Dokko and K. Kanamura, *J. Power Sources*, 2005, **146**, 555–558.
69 M. H. Lee, J. Y. Kim and H. K. Song, *Chem. Commun.*, 2010, **46**, 6795–6797.
70 R. Yang, X. P. Song, M. S. Zhao and F. Wang, *J. Alloys Compd.*, 2009, **468**, 365–369.
71 D. H. Kim and J. Kim, *Electrochem. Solid-State Lett.*, 2006, **9**, A439–A442.
72 K. T. Lee, W. H. Kan and L. F. Nazar, *J. Am. Chem. Soc.*, 2009, **131**, 6044.

73 S. K. Martha, B. Markovsky, J. Grinblat, Y. Gofer, O. Haik, E. Zinigrad, D. Aurbach, T. Drezen, D. Wang, G. Deghenghi and I. Exnar, *J. Electrochem. Soc.*, 2009, **156**, A541–A552.
74 D. Y. Wang, H. Buqa, M. Crouzet, G. Deghenghi, T. Drezen, I. Exnar, N. H. Kwon, J. H. Miners, L. Poletto and M. Graetzel, *J. Power Sources*, 2009, **189**, 624–628.
75 N. Recham, M. Armand and J. M. Tarascon, *C. R. Chim.*, 2010, **13**, 106–116.
76 M. Nakayama, S. Goto, Y. Uchimoto, M. Wakihara and Y. Kitajima, *Chem. Mater.*, 2004, **16**, 3399–3401.
77 A. K. Padhi, K. S. Nanjundaswamy, C. Masquelier, S. Okada and J. B. Goodenough, *J. Electrochem. Soc.*, 1997, **144**, 1609–1613.
78 S. Y. Chung, J. T. Bloking and Y. M. Chiang, *Nat. Mater.*, 2002, **1**, 123–128.
79 A. Yamada and S. C. Chung, *J. Electrochem. Soc.*, 2001, **148**, A960–A967.
80 P. Tang and N. A. W. Holzwarth, *Phys. Rev. B: Condens. Matter*, 2003, **68**, 10.
81 F. Zhou, K. S. Kang, T. Maxisch, G. Ceder and D. Morgan, *Solid State Commun.*, 2004, **132**, 181–186.
82 Z. L. Wang, S. R. Sun, D. G. Xia, W. S. Chu, S. Zhang and Z. Y. Wu, *J. Phys. Chem. C*, 2008, **112**, 17450–17455.
83 J. Xu and G. Chen, *Phys. B*, 2010, **405**, 803–807.
84 L. Castro, R. Dedryvere, M. El Khalifi, P. E. Lippens, J. Breger, C. Tessier and D. Gonbeau, *J. Phys. Chem. C*, 2010, **114**, 17995–18000.
85 S. Q. Wu, Z. Z. Zhu, Y. Yang and Z. F. Hou, *Comput. Mater. Sci.*, 2009, **44**, 1243–1251.
86 P. Larsson, R. Ahuja, A. Nyten and J. O. Thomas, *Electrochem. Commun.*, 2006, **8**, 797–800.
87 G. H. Zhong, Y. L. Li, P. Yan, Z. Liu, M. H. Xie and H. Q. Lin, *J. Phys. Chem. C*, 2010, **114**, 3693–3700.
88 Z. J. Liu and X. J. Huang, *Solid State Ionics*, 2010, **181**, 1209–1213.
89 A. Kokalj, R. Dominko, G. Mali, A. Meden, M. Gaberscek and J. Jamnik, *Chem. Mater.*, 2007, **19**, 3633–3640.
90 K. Zaghib, A. Mauger, J. B. Goodenough, F. Gendron and C. M. Julien, *Chem. Mater.*, 2007, **19**, 3740–3747.
91 F. Zhou, M. Cococcioni, C. A. Marianetti, D. Morgan and G. Ceder, *Phys. Rev. B*, 2004, **70**, 8.
92 Y. S. Meng and M. E. Arroyo-de Dompablo, *Energy Environ. Sci.*, 2009, **2**, 589–609.
93 V. I. Anisimov, J. Zaanen and O. K. Andersen, *Phys. Rev. B: Condens. Matter*, 1991, **44**, 943.
94 B. L. Ellis, K. T. Lee and L. F. Nazar, *Chem. Mater.*, 2010, **22**, 691–714.
95 Z. H. Li, D. M. Zhang and F. X. Yang, *J. Mater. Sci.*, 2009, **44**, 2435–2443.
96 J. W. Fergus, *J. Power Sources*, 2010, **195**, 939–954.
97 M. S. Whittingham, Y. N. Song, S. Lutta, P. Y. Zavalij and N. A. Chernova, *J. Mater. Chem.*, 2005, **15**, 3362–3379.
98 A. Yamada, M. Hosoya, S. C. Chung, Y. Kudo, K. Hinokuma, K. Y. Liu and Y. Nishi, *J. Power Sources*, 2003, **119–121**, 232–238.
99 W. J. Zhang, *J. Electrochem. Soc.*, 2010, **157**, A1040–A1046.
100 S. Franger, C. Benoit, C. Bourbon and F. Le Cras, *J. Phys. Chem. Solids*, 2006, **67**, 1338–1342.
101 P. P. Prosini, M. Lisi, D. Zane and M. Pasquali, *Solid State Ionics*, 2002, **148**, 45–51.
102 K. S. Park, A. Benayad, M. S. Park, A. Yamada and S. G. Doo, *Chem. Commun.*, 2010, **46**, 2572–2574.
103 A. Yamada, Y. Kudo and K. Y. Liu, *J. Electrochem. Soc.*, 2001, **148**, A747–A754.
104 C. M. Doherty, R. A. Caruso and C. J. Drummond, *Energy Environ. Sci.*, 2010, **3**, 813–823.
105 S. Q. Shi, L. J. Liu, C. Y. Ouyang, D. S. Wang, Z. X. Wang, L. Q. Chen and X. J. Huang, *Phys. Rev. B*, 2003, **68**, 5.
106 M. S. Islam, D. J. Driscoll, C. A. J. Fisher and P. R. Slater, *Chem. Mater.*, 2005, **17**, 5085–5092.
107 N. J. Yun, H. W. Ha, K. H. Jeong, H. Y. Park and K. Kim, *J. Power Sources*, 2006, **160**, 1361–1368.
108 Y. K. Zhou, J. Wang, Y. Y. Hu, R. O'Hayre and Z. P. Shao, *Chem. Commun.*, 2010, **46**, 7151–7153.
109 Z. H. Chen and J. R. Dahn, *J. Electrochem. Soc.*, 2002, **149**, A1184–A1189.
110 M. M. Doeff, Y. Q. Hu, F. McLarnon and R. Kostecki, *Electrochem. Solid-State Lett.*, 2003, **6**, A207–A209.
111 R. Dominko, M. Bele, M. Gaberscek, M. Remskar, D. Hanzel, S. Pejovnik and J. Jamnik, *J. Electrochem. Soc.*, 2005, **152**, A607–A610.
112 Y. Q. Hu, M. M. Doeff, R. Kostecki and R. Finones, *J. Electrochem. Soc.*, 2004, **151**, A1279–A1285.
113 M. M. Doeff, J. D. Wilcox, R. Kostecki and G. Lau, *J. Power Sources*, 2006, **163**, 180–184.
114 J. D. Wilcox, M. M. Doeff, M. Marcinek and R. Kostecki, *J. Electrochem. Soc.*, 2007, **154**, A389–A395.
115 F. Croce, A. D. Epifanio, J. Hassoun, A. Deptula, T. Olczac and B. Scrosati, *Electrochem. Solid-State Lett.*, 2002, **5**, A47–A50.
116 K. S. Park, J. T. Son, H. T. Chung, S. J. Kim, C. H. Lee, K. T. Kang and H. G. Kim, *Solid State Commun.*, 2004, **129**, 311–314.
117 K. S. Park, S. B. Schougaard and J. B. Goodenough, *Adv. Mater.*, 2007, **19**, 848.
118 I. Boyano, J. A. Blazquez, I. de Meatza, M. Bengoechea, O. Miguel, H. Grande, Y. H. Huang and J. B. Goodenough, *J. Power Sources*, 2010, **195**, 5351–5359.
119 B. Kang and G. Ceder, *Nature*, 2009, **458**, 190–193.
120 G. Ceder and B. Kang, *J. Power Sources*, 2009, **194**, 1024–1028.
121 K. Zaghib, J. B. Goodenough, A. Mauger and C. Julien, *J. Power Sources*, 2009, **194**, 1021–1023.
122 M. H. Liang and L. J. Zhi, *J. Mater. Chem.*, 2009, **19**, 5871–5878.
123 D. Chen, L. H. Tang and J. H. Li, *Chem. Soc. Rev.*, 2010, **39**, 3157–3180.
124 E. Yoo, J. Kim, E. Hosono, H. Zhou, T. Kudo and I. Honma, *Nano Lett.*, 2008, **8**, 2277–2282.
125 S. M. Paek, E. Yoo and I. Honma, *Nano Lett.*, 2009, **9**, 72–75.
126 S. B. Yang, X. L. Feng, S. Ivanovici and K. Mullen, *Angew. Chem., Int. Ed.*, 2010, **49**, 8408–8411.
127 D. H. Wang, D. W. Choi, J. Li, Z. G. Yang, Z. M. Nie, R. Kou, D. H. Hu, C. M. Wang, L. V. Saraf, J. G. Zhang, I. A. Aksay and J. Liu, *ACS Nano*, 2009, **3**, 907–914.
128 X. F. Zhou, F. Wang, Y. M. Zhu and Z. P. Liu, *J. Mater. Chem.*, 2011, **21**, 3353–3358.
129 Y. Ding, Y. Jiang, F. Xu, J. Yin, H. Ren, Q. Zhuo, Z. Long and P. Zhang, *Electrochem. Commun.*, 2010, **12**, 10–13.
130 F. Y. Su, C. H. You, Y. B. He, W. Lv, W. Cui, F. M. Jin, B. H. Li, Q. H. Yang and F. Y. Kang, *J. Mater. Chem.*, 2010, **20**, 9644–9650.
131 L. Wang, H. B. Wang, Z. H. Liu, C. Xiao, S. M. Dong, P. X. Han, Z. Y. Zhang, X. Y. Zhang, C. F. Bi and G. L. Cui, *Solid State Ionics*, 2010, **181**, 1685–1689.
132 M. M. Doeff, J. D. Wilcox, R. Yu, A. Aumentado, M. Marcinek and R. Kostecki, *J. Solid State Electrochem.*, 2007, **12**, 995–1001.
133 Y. M. Chiang, N. Meethong and Y. H. Kao, *Adv. Funct. Mater.*, 2010, **20**, 189–191.
134 N. Meethong, Y. H. Kao, S. A. Speakman and Y. M. Chiang, *Adv. Funct. Mater.*, 2009, **19**, 1060–1070.
135 N. Meethong, H. Y. S. Huang, W. C. Carter and Y. M. Chiang, *Electrochem. Solid-State Lett.*, 2007, **10**, A134–A138.
136 N. Meethong, Y. H. Kao, W. C. Carter and Y. M. Chiang, *Chem. Mater.*, 2010, **22**, 1088–1097.
137 N. Ravet, A. Abouimrane and M. Armand, *Nat. Mater.*, 2003, **2**, 702–702.
138 P. S. Herle, B. Ellis, N. Coombs and L. F. Nazar, *Nat. Mater.*, 2004, **3**, 147–152.
139 B. Ellis, P. S. Herle, Y. H. Rho, L. F. Nazar, R. Dunlap, L. K. Perry and D. H. Ryan, *Faraday Discuss.*, 2007, **134**, 119–141.
140 M. Wagemaker, B. L. Ellis, D. Luetzenkirchen-Hecht, F. M. Mulder and L. F. Nazar, *Chem. Mater.*, 2008, **20**, 6313–6315.
141 B. L. Ellis, M. Wagemaker, F. M. Mulder and L. F. Nazar, *Adv. Funct. Mater.*, 2010, **20**, 186–188.
142 C. A. J. Fisher, V. M. H. Prieto and M. S. Islam, *Chem. Mater.*, 2008, **20**, 5907–5915.
143 V. Srinivasan and J. Newman, *J. Electrochem. Soc.*, 2004, **151**, A1517–A1529.
144 A. Yamada, H. Koizumi, S. I. Nishimura, N. Sonoyama, R. Kanno, M. Yonemura, T. Nakamura and Y. Kobayashi, *Nat. Mater.*, 2006, **5**, 357–360.
145 C. Delacourt, P. Poizot, J. M. Tarascon and C. Masquelier, *Nat. Mater.*, 2005, **4**, 254–260.
146 P. Gibot, M. Casas-Cabanas, L. Laffont, S. Levasseur, P. Carlach, S. Hamelet, J. M. Tarascon and C. Masquelier, *Nat. Mater.*, 2008, **7**, 741–747.
147 G. Kobayashi, S. I. Nishimura, M. S. Park, R. Kanno, M. Yashima, T. Ida and A. Yamada, *Adv. Funct. Mater.*, 2009, **19**, 395–403.

148 D. Burch and M. Z. Bazant, *Nano Lett.*, 2009, **9**, 3795–3800.
149 D. Morgan, A. Van der Ven and G. Ceder, *Electrochem. Solid-State Lett.*, 2004, **7**, A30–A32.
150 S. Nishimura, G. Kobayashi, K. Ohoyama, R. Kanno, M. Yashima and A. Yamada, *Nat. Mater.*, 2008, **7**, 707–711.
151 P. X. Zhang, Y. P. Wu, D. Y. Zhang, Q. M. Xu, J. H. Liu, X. Z. Ren, Z. K. Luo, M. L. Wang and W. L. Hong, *J. Phys. Chem. A*, 2008, **112**, 5406–5410.
152 L. Laffont, C. Delacourt, P. Gibot, M. Y. Wu, P. Kooyman, C. Masquelier and J. M. Tarascon, *Chem. Mater.*, 2006, **18**, 5520–5529.
153 G. Y. Chen, X. Y. Song and T. J. Richardson, *Electrochem. Solid-State Lett.*, 2006, **9**, A295–A298.
154 A. S. Andersson and J. O. Thomas, *J. Power Sources*, 2001, **97–98**, 498–502.
155 C. Delmas, M. Maccario, L. Croguennec, F. Le Cras and F. Weill, *Nat. Mater.*, 2008, **7**, 665–671.
156 C. Delacourt, L. Laffont, R. Bouchet, C. Wurm, J. B. Leriche, M. Morcrette, J. M. Tarascon and C. Masquelier, *J. Electrochem. Soc.*, 2005, **152**, A913–A921.
157 C. Delacourt, P. Poizot, M. Morcrette, J. M. Tarascon and C. Masquelier, *Chem. Mater.*, 2004, **16**, 93–99.
158 J. S. Yang and J. J. Xu, *J. Electrochem. Soc.*, 2006, **153**, A716–A723.
159 N. H. Kwon, T. Drezen, I. Exnar, I. Teerlinck, M. Isono and M. Graetzel, *Electrochem. Solid-State Lett.*, 2006, **9**, A277–A280.
160 H. S. Fang, L. P. Li, Y. Yang, G. F. Yan and G. S. Li, *Chem. Commun.*, 2008, 1118–1120.
161 Z. Bakenov and I. Taniguchi, *Electrochem. Commun.*, 2010, **12**, 75–78.
162 D. W. Choi, D. H. Wang, I. T. Bae, J. Xiao, Z. M. Nie, W. Wang, V. V. Viswanathan, Y. J. Lee, J. G. Zhang, G. L. Graff, Z. G. Yang and J. Liu, *Nano Lett.*, 2010, **10**, 2799–2805.
163 G. Y. Chen, J. D. Wilcox and T. J. Richardson, *Electrochem. Solid-State Lett.*, 2008, **11**, A190–A194.
164 J. W. Lee, M. S. Park, B. Anass, J. H. Park, M. S. Paik and S. G. Doo, *Electrochim. Acta*, 2010, **55**, 4162–4169.
165 Z. Bakenov and I. Taniguchi, *J. Electrochem. Soc.*, 2010, **157**, A430–A436.
166 T. Shiratsuchi, S. Okada, T. Doi and J. Yamaki, *Electrochim. Acta*, 2009, **54**, 3145–3151.
167 N. Meethong, Y. H. Kao, M. Tang, H. Y. Huang, W. C. Carter and Y. M. Chiang, *Chem. Mater.*, 2008, **20**, 6189–6198.
168 N. Meethong, H. Y. S. Huang, S. A. Speakman, W. C. Carter and Y. M. Chiang, *Adv. Funct. Mater.*, 2007, **17**, 1115–1123.
169 N. N. Bramnik, K. Nikolowski, C. Baehtz, K. G. Bramnik and H. Ehrenberg, *Chem. Mater.*, 2007, **19**, 908–915.
170 H. Ehrenberg, N. N. Bramnik, A. Senyshyn and H. Fuess, *Solid State Sci.*, 2009, **11**, 18–23.
171 N. N. Bramnik, K. Nikolowski, D. M. Trots and H. Ehrenberg, *Electrochem. Solid-State Lett.*, 2008, **11**, A89–A93.
172 M. Armand, C. Michot, N. Ravet, M. Simoneau and P. Hovington, U.S. Patent 6 085 015, 2000.
173 A. R. West and P. G. Bruce, *Acta Crystallogr., Sect. B: Struct. Crystallogr. Cryst. Chem.*, 1982, **38**, 1891–1896.
174 A. R. West, *Z. Kristallogr., Kristallgeom., Kristallphys., Kristallchem.*, 1975, **141**, 422–436.
175 C. Sirisopanaporn, A. Boulineau, D. Hanzel, R. Dominko, B. Budic, A. R. Armstrong, P. G. Bruce and C. Masquelier, *Inorg. Chem.*, 2010, **49**, 7446–7451.
176 S. I. Nishimura, S. Hayase, R. Kanno, M. Yashima, N. Nakayama and A. Yamada, *J. Am. Chem. Soc.*, 2008, **130**, 13212–13213.
177 A. Boulineau, C. Sirisopanaporn, R. Dominko, A. R. Armstrong, P. G. Bruce and C. Masquelier, *Dalton Trans.*, 2010, **39**, 6310–6316.
178 M. E. Arroyo-DeDompablo, R. Dominko, J. M. Gallardo-Amores, L. Dupont, G. Mali, H. Ehrenberg, J. Jamnik and E. Moran, *Chem. Mater.*, 2008, **20**, 5574–5584.
179 V. V. Politaev, A. A. Petrenko, V. B. Nalbandyan, B. S. Medvedev and E. S. Shvetsova, *J. Solid State Chem.*, 2007, **180**, 1045–1050.
180 H. Yamaguchi, K. Akatsuka, M. Setoguchi and Y. Takaki, *Acta Crystallogr., Sect. B: Struct. Crystallogr. Cryst. Chem.*, 1979, **35**, 2680–2682.
181 M. de Dompablo, U. Amador, J. M. Gallardo-Amores, E. Moran, H. Ehrenberg, L. Dupont and R. Dominko, *J. Power Sources*, 2009, **189**, 638–642.
182 G. Mali, A. Meden and R. Dominko, *Chem. Commun.*, 2010, **46**, 3306–3308.
183 A. R. Armstrong, C. Lyness, M. Menetrier and P. G. Bruce, *Chem. Mater.*, 2010, **22**, 1892–1900.
184 K. Zaghib, A. A. Salah, N. Ravet, A. Mauger, F. Gendron and C. M. Julien, *J. Power Sources*, 2006, **160**, 1381–1386.
185 I. Belharouak, A. Abouimrane and K. Amine, *J. Phys. Chem. C*, 2009, **113**, 20733–20737.
186 Z. L. Gong, Ph.D. Thesis, Xiamen Univesrsity, Xiamen, China, 2007.
187 A. Nyten, S. Kamali, L. Haggstrom, T. Gustafsson and J. O. Thomas, *J. Mater. Chem.*, 2006, **16**, 2266–2272.
188 R. Dominko, *J. Power Sources*, 2008, **184**, 462–468.
189 R. Dominko, D. E. Conte, D. Hanzel, M. Gaberscek and J. Jamnik, *J. Power Sources*, 2008, **178**, 842–847.
190 S. Zhang, C. Deng and S. Y. Yang, *Electrochem. Solid-State Lett.*, 2009, **12**, A136–A139.
191 N. Yabuuchi, Y. Yamakawa, K. Yoshii and S. Komaba, *Electrochemistry*, 2010, **78**, 363–366.
192 D. P. Lv, X. K. Huang, W. Wen, Y. X. Li and Y. Yang, *15th International Meeting on Lithium Batteries*, Abstract #497, June 27-July 2, 2010, Montreal, Canada.
193 D. P. Lv, X. K. Huang, W. Wen, Y. X. Li and Y. Yang, *15th International Meeting on Lithium Batteries*, Abstract #498, June 27-July 2, 2010, Montreal, Canada.
194 A. Nyten, M. Stjerndahl, H. Rensmo, H. Siegbahn, M. Armand, T. Gustafsson, K. Edstrom and J. O. Thomas, *J. Mater. Chem.*, 2006, **16**, 3483–3488.
195 D. Ensling, M. Stjerndahl, A. Nyten, T. Gustafsson and J. O. Thomas, *J. Mater. Chem.*, 2009, **19**, 82–88.
196 Z. L. Gong, Y. X. Li and Y. Yang, *Electrochem. Solid-State Lett.*, 2006, **9**, A542–A544.
197 R. Dominko, M. Bele, A. Kokalj, M. Gaberscek and J. Jamnik, *J. Power Sources*, 2007, **174**, 457–461.
198 P. Larsson, R. Ahuja, A. Liivat and J. O. Thomas, *Comput. Mater. Sci.*, 2010, **47**, 678–684.
199 S. Q. Wu, J. H. Zhang, Z. Z. Zhu and Y. Yang, *Curr. Appl. Phys.*, 2007, **7**, 611–616.
200 M. de Dompablo, J. M. Gallardo-Amores, J. Garcia-Martinez, E. Moran, J. M. Tarascon and M. Armand, *Solid State Ionics*, 2008, **179**, 1758–1762.
201 N. Kuganathan and M. S. Islam, *Chem. Mater.*, 2009, **21**, 5196–5202.
202 A. Liivat and J. O. Thomas, *Solid State Ionics*, 2009, DOI: 10.1016/j.ssi.2009.1012.1009.
203 A. Liivat and J. O. Thomas, *Computational Materials Science*, 2010, DOI: 10.1016/j.commatsci.2010.1007.1025.
204 J. Barker, M. Y. Saidi, R. K. B. Gover, P. Burns and A. Bryan, *J. Power Sources*, 2007, **174**, 927–931.
205 J. Barker, R. K. B. Gover, P. Burns and A. J. Bryan, *Electrochem. Solid-State Lett.*, 2007, **10**, A130–A133.
206 J. Barker, R. K. B. Gover, P. Burns, A. Bryan, M. Y. Saidi and J. L. Swoyer, *J. Power Sources*, 2005, **146**, 516–520.
207 J. Barker, R. K. B. Gover, P. Burns, A. Bryan, M. Y. Saidi and J. L. Swoyer, *J. Electrochem. Soc.*, 2005, **152**, A1776–A1779.
208 J. L. Pizarrosanz, J. M. Dance, G. Villeneuve and M. I. Arriortuamarcaida, *Mater. Lett.*, 1994, **18**, 327–330.
209 J. Barker, M. Y. Saidi and J. L. Swoyer, *Electrochem. Solid-State Lett.*, 2003, **6**, A1–A4.
210 J. Barker, R. K. B. Gover, P. Burns and A. J. Bryan, *J. Electrochem. Soc.*, 2007, **154**, A882–A887.
211 M. Ramzan, S. Lebegue and R. Ahuja, *Appl. Phys. Lett.*, 2009, **94**, 3.
212 G. Armstrong, A. R. Armstrong, P. G. Bruce, P. Reale and B. Scrosati, *Adv. Mater.*, 2006, **18**, 2597.
213 P. Reale, S. Panero and B. Scrosati, *J. Electrochem. Soc.*, 2005, **152**, A1949–A1954.
214 P. Reale, S. Panero, B. Scrosati, J. Garche, M. Wohlfahrt-Mehrens and M. Wachtler, *J. Electrochem. Soc.*, 2004, **151**, A2138–A2142.
215 L. Sebastian, J. Gopalakrishnan and Y. Piffard, *J. Mater. Chem.*, 2002, **12**, 374–377.
216 J. L. Allen, K. Xu, S. S. Zhang and T. R. Jow, in *Materials for Energy Storage, Generation and Transport*, ed. R. B. Schwarz, G. Ceder and S. A. Ringel, Materials Research Society, Warrendale, 2002, vol. 730, pp. 9–14.

217 V. Aravindan, K. Karthikeyan, S. Amaresh and Y. S. Lee, *Bull. Korean Chem. Soc.*, 2010, **31**, 1506–1508.
218 L. Chen, Y. M. Zhao, X. N. An, J. M. Liu, Y. Z. Dong, Y. H. Chen and Q. Kuang, *J. Alloys Compd.*, 2010, **494**, 415–419.
219 K. M. Begam, M. S. Michael and S. R. S. Prabaharan, *J. Solid State Electrochem.*, 2007, **12**, 971–977.
220 M. E. Arroyo-de Dompablo, U. Amador, M. Alvarez, J. M. Gallardo and F. Garcia-Alvarado, *Solid State Ionics*, 2006, **177**, 2625–2628.
221 M. E. Arroyo-de Dompablo, U. Amador and F. Garcia-Alvarado, *J. Electrochem. Soc.*, 2006, **153**, A673–A678.
222 M. Kishore and U. V. Varadaraju, *Mater. Res. Bull.*, 2006, **41**, 601–607.
223 S. R. S. Prabaharan, M. S. Michael and K. M. Begam, *Electrochem. Solid-State Lett.*, 2004, **7**, A416–A420.
224 S. R. S. Prabaharan, M. S. Michael, S. Ramesh and K. M. Begam, *J. Electroanal. Chem.*, 2004, **570**, 107–112.
225 K. M. Begam, M. S. Michael, Y. H. Taufiq-Yap and S. R. S. Prabaharan, *A new electrode with polyanion - (MoO43) as cathode forlithium ion batteries*, 2002.
226 K. M. Begam, M. S. Michael, Y. H. Taufiq-Yap and S. R. S. Prabaharan, *Electrochem. Solid-State Lett.*, 2004, **7**, A242–A246.
227 K. M. Begam, M. S. Michael and S. R. S. Prabaharan, *Ionics*, 2007, **13**, 467–471.
228 M. Alvarez-Vega, U. Amador and M. E. Arroyo-de Dompablo, *J. Electrochem. Soc.*, 2005, **152**, A1306–A1311.
229 M. de Dompablo, M. Alvarez-Vera, C. Baehtz and U. Amador, *J. Electrochem. Soc.*, 2006, **153**, A275–A281.
230 D. Mikhailova, A. Sarapulova, A. Voss, A. Thomas, S. Oswald, W. Gruner, D. M. Trots, N. N. Bramnik and H. Ehrenberg, *Chem. Mater.*, 2010, **22**, 3165–3173.
231 C. L. Li and Z. W. Fu, *Electrochim. Acta*, 2008, **53**, 6434–6443.
232 C. L. Li and Z. W. Fu, *Electrochim. Acta*, 2008, **53**, 4293–4301.

